Hydrology Research

British Hydrological Society

IWA PUBLISHING

Hydrology Research Vol 55 No 3, 351 doi: 10.2166/nh.2024.169

Assessment of anthropogenic and climate-driven water storage variations over water-stressed river basins of Ethiopia

Agegnehu Kitanbo Yoshe [a,b]

[a] Department of Water Resources and Irrigation Engineering, Arba Minch University, 21 Post Office Box, Arba Minch, Ethiopia
[b] Department of Water Supply, Sewerage, Construction Systems of Water Resources Protection, Irkutsk National Research Technical University, Irkutsk, Russia
E-mail: agegnehu.kitanbo@amu.edu.et

AKY, 0000-0002-3792-5854

ABSTRACT

Globally, surface water, groundwater, soil moisture, snow storage, canopy water, and wet biomass constituents make up water storage, which plays a significant role in the hydrological water balance. Evaluating the variations in water storage anomalies associated with climate forcing and human activities over river basins is crucial for assessing water scarcity and predicting potential pressures on water resources in the future. In this study, we assessed the impacts of climatic and anthropogenic drivers on the change in water storage in the river basins of Ethiopia by using the independent component analysis to examine Gravity Recovery and Climate Experiment with the Global Land Data Assimilate System-based water storage and comparing the independent component analysis with hydro-meteorological data and statistical data related to human activities. It is of great significance for helping people better understand the evaluation of terrestrial water storage anomalies under the combined influence of climatic change and anthropogenic activities and providing information for better protection and utilization of water resources at river basin level. It is crucial to take effective measures to protect these precious land and water resources and prevent their further deterioration. The estimated result will be essential for sustainable water management and protection.

Key words: climatic and anthropologic factors, GLDAS and GRACE dataset, power dataset, evapotransipiration, water storage variation

HIGHLIGHTS

- Characteristics of water storage variation was analysed over each river basin.
- The impact of climatic change and human activities on water storage was evaluated.
- Independent component analysis was performed on terrestrial water storage anomalies for each river basin and obtained two leading modes (the trend and annual modes).
- The intensity of human activities has increased over each river basins.
- Climate change is the dominant factor observed during the study period.

1. INTRODUCTION

Freshwater resources are critical ecosystems that support human and animal life (Geda *et al.* 2020). The availability of water is a critical issue that is used in different sectors of the world that serve indirectly or directly throughout the lifetime of human beings. This includes hydroelectric energy production, water supply for drinking, irrigating agriculture, transportation, industrial water supply, and others. Due to that, the demand for water has been rising all over the world (Singh *et al.* 2014, 2017). For efficient utilization of surface water resources that are available at balanced extents to increase economic, environmental, and social benefits, it is important to understand available water resources. Estimating the water balance means assessing the needs, current condition, and trends of the water resources on the land surface, which strengthens decision-making for water resource management and is said to be pricing. The role of opening an inclusive strategy for optimization and management of water resources to manage demand was to reduce the limit of the water problem by identifying its balance (Belkhiri *et al.* 2018).

Currently, different scholars are focused on water balance assessment around the world by using different models like Arc Soil and Water Assessment Tool (SWAT) and WEAP (Kumar *et al.* 2018). According to Gupta *et al.* (2014), the

availability of water resources in large river basins is the current topic for discussion. Assessment of the availability of water storage was very essential for water resource planning and management. They focused on the Narmada River Basin located in India to evaluate its water availability by using an integrated approach of remote sensing and GIS tools and techniques. An evaluation of the water budget at the heart of southwestern Ontario, located in central Canada, including all drainage areas for the Grand River and its contributors, was carried out to develop scenarios for future weather conditions by using global circulation models (Golmohammadi *et al.* 2017). Estimation of water balance for the Chirchik River Basin in northeastern Uzbekistan was performed by using the integrated Mike SHE models to generate quantitative results of the river (Usmanov *et al.* 2016). Raghavendra & Cholke (2017) evaluated continental evapotranspiration by using Gravity Recovery and Climate Experiment (GRACE) in the Australian Semi-Arid Basins, which is a recently developed land surface model to assess water balance. Water balance is based on conservation of the law of mass, which shows that any change in the water content of a given soil volume during a specified period must equal the difference between the amount of water added to the soil volume and the amount of water withdrawn from it. It also helps to quantify the relationship between precipitation, evaporation, evapotranspiration, and aquifer draft and provides a framework for the future planning of sustainable exploitation of the available water resources (Kanga 2017). Based on water balance models, the water balance components have been evaluated at diverse scales in recent years. For example, McCabe & Wolock (2013) assess the mechanism of water balance at the global scale, and Herrmann *et al.* (2015) assess the spatial variation of water balance components at the regional level. Generally, researchers have mostly focused on the estimation of water balance components at basin or watershed levels (White *et al.* 2011; Gunkel *et al.* 2015; Uniyal *et al.* 2015). Different findings have been discussed on water balance through parameters like vegetation patterns, land cover types, and ecosystem level. For example, quantifying the change of every water balance component in a small watershed with diverse land cover types (Jian *et al.* 2015), Thompson *et al.* (2011) evaluated the spatial scale dependency of ecohydrologically mediated water balance partitioning for catchment ecohydrology using a simple model of water balance and vegetation coupling on a hierarchical flow path network and reported that the generated spatial dependency in a really averaged hydrological variables, water balance, and parameters describing hydrological partitioning provides a theoretical approach to connect water balance at patch and catchment scales. Jasrotia *et al.* (2009) estimated the moisture deficit and watershed moisture surplus by using remote sensing and the ArcGIS approach. A spatial semi-distribution of water balance model was developed to simulate the mean monthly hydrological process by using the soil conservation service curve numbers (Jenifa *et al.* 2010). The water balance of river basins was analyzed and quantified by the Arc SWAT model (Sathian 2009). Stream flow, water balance, and monthly inflow volume were simulated to predict water balance components by Arc SWAT (Pagliero *et al.* 2014).

Ethiopia is gifted by a natural water resource called the water tower of East Africa, due to water availability in the country, but there are water shortages in the areas of water supply, irrigation, and depending on a rain-fed agricultural system due to lack of proper utilization and exploitation of this natural resource of water. According to Awulachew *et al.* (2007), 560 irrigation potential sites were identified, and it was estimated that about 3.7 million hectares of land were available for irrigation in Ethiopia by the Ministry of Water Resources. Water availability was essential for irrigation (Bayissa *et al.* 2017; Tiri *et al.* 2018; Alemu *et al.* 2022). The economic growth of Ethiopia is growing at the fastest rate and is facing greater challenges to meet energy demands that come from household consumption, the industrial system, and service sectors. To meet the energy demand, mega hydropower projects are constructed on main river basins (Degefu *et al.* 2015). The national water resources are estimated to have the potential to generate as much as 30,000 MW of power from economically feasible hydropower projects (World Bank 2013). There are nearly 200 identified economically feasible sites for hydropower development in the country (Bartle 2002). The construction of Sugar Industries is growing. The availability of high-potential water leads us to create a good environment for the future in different directions, not only for hydropower generation but also for generating incomes due to indirect additional functions of water based on fish production, tourism, water supply, irrigation, and others (Degefu *et al.* 2015).

Due to the second phase of growth and transformation, the economic growth of the country was growing at a high rate because of the fast industrial growth, which led to manufacturing subsectors (Altaseb & Singh 2018). This second phase of growth and transformation is targeted at improving the number and productivity of manufacturing industries, supported by the government, to increase the growth of physical infrastructure through public investment projects in water resource basins and other areas, to feed this increasing population, to meet the high demand for hydropower, to produce maximum production by irrigation agriculture, and to increase industrialization, which leads to high demand for water in the country.

According to Abboye (2021), the Ethiopian government's food self-sufficiency policy program, improving the productivity and production of bread wheat as well as facilitating its marketing access, is one of the key parts of the economic growth strategies. Due to that, understanding the current condition of water availability at river basin level was the main issue in the country for optimization and management of water resources to identify different demands related to water and to reduce water crises that were happening because of underutilization of water resources.

Spatiotemporal variation in its water storage capacity has a major impact on the socioeconomic development and livelihood of the country. Frequent natural disasters are mainly represented by large-scale and long-term drought and regional floods, which are generally linked to abnormal terrestrial water dynamics (Thomas *et al.* 2014; Xu *et al.* 2019). However, the lack of *in situ* observation limits our understanding of the water cycle in this region. Fortunately, studies have reported that the terrestrial water storage derived from GRACE satellite data shows both the potential for revealing variation in surface water storage and the ability to support large-scale hydrological modeling (Klees *et al*. 2007; Luo *et al.* 2016; Yang *et al.* 2017; Zhao & Li 2017; Frappart & Ramillien 2018; Yoshe 2023). Studies show that GRACE has displayed satisfactory results for terrestrial water storage (Li *et al.* 2013, 2018; Ni *et al.* 2014; Feng *et al.* 2017; Khaki *et al.* 2018; Wang *et al*. 2019). There are no studies on characterizing terrestrial water storage and factors that lead to variation in water storage based on the GRACE dataset and Global Land Data Assimilation System (GLDAS) model on the major river basin of Ethiopia, for example, Awulachew *et al.* (2007) focused on annual flow of the major river basin, but neglecting the spatial heterogeneity of terrestrial water storage changes. Generally, the spatiotemporal variations of terrestrial water storage and its changes are the result of the combined effect of climate change and human activities (Hu *et al.* 2018). Precipitation, runoff, and evapotranspiration are dominating processes of change in terrestrial water storage either in space and/or time (Tangdamrongsub *et al.* 2011; Frappart *et al.* 2013; Yang *et al.* 2015). Anthropogenic processes like irrigation, the abstraction of groundwater, and land use influence terrestrial water storage in highly populated areas (De Beurs *et al.* 2015; Huang *et al.* 2015; Khandu *et al.* 2016). Each river basin has its own particular local climates, relief conditions, and human conditions, and some of these factors affect the evaluation of terrestrial water storage. Generally, the water storage estimate provided by GRACE and GLDAS is comprehensively affected by human activities and climatic changes, and climatic change may cause us to underestimate or overestimate the impact of human activities on water storage in different periods (Chen *et al.* 2016; Humphrey *et al.* 2017; Humphrey & Gudmundsson 2019; Zhong *et al.* 2019; Liu *et al.* 2021). It is difficult to isolate the impact of climate change and human activities on water storage derived from GRACE and GLDAS observations. Many studies have attempted to assess the relative contribution of natural and anthropogenic effects on water storage (Fasullo *et al.* 2016; Felfelani *et al.* 2017; Zhong *et al.* 2019). Felfelani *et al.* (2017) isolated natural and human-induced changes in water storage by comparing results from different hydrological model simulations and GRACE data over large basins. Yi *et al.* (2016) analyzed the impact of human activities and climate driving on water storage by establishing a linear relationship between variation in precipitation and water storage, assuming that the impact of human activities on terrestrial water storage is constant over time. Zhong *et al.* (2019) quantified the contribution of climate-driven water storage and its long-term trends based on the reconstruction of long-term climate-driven water storage variations. These studies were primarily conducted based on hydrological models or established statistical models that simulate natural, dynamically driven changes in water storage to reconstruct climate-driven water storage anomalies. However, due to the uncertainty of state-of-the-art hydrological models and forcing datasets, the impact of human intervention on terrestrial water storage may be underestimated or overestimated (Scanlon *et al.* 2018). The primary objective of this article is to explore the potential driving factors for the change in terrestrial water storage in Ethiopian river basins. To do so, we conduct a comprehensive analysis of the terrestrial water storage from GLDAS and GRACE in the major river basin of Ethiopia based on the independent component analysis (ICA). First, we investigate the water storage changes in the major river basins of Ethiopia from GRACE and GLDAS, and then we decompose the terrestrial water storage using the ICA technique to illuminate the spatiotemporal patterns of water storage variations in the major river basins of Ethiopia. Finally, we compare the ICA modes with hydrological model data, ground statistics data (coal mining, irrigation, grazing, etc.), and simulated climatic water storage anomalies products derived from the statistical model proposed by Humphrey to explain the meaning of each dominant signal that separates through ICA results (Sun *et al.* 2020). This will improve our understanding of the various factors affecting basin water storage, including anthropogenic and climate-driven water storage variations. To date, no such investigation has been available in the existing literature for Ethiopia at the river basin level. Therefore, adopted approaches for long-term availability of water storage and its result will be regarded as a new and honest contribution to Ethiopia's river basins.

2. MATERIALS AND METHODS

2.1. Description of the study

Ethiopia is located between 3°N–15°N and 33°E–48°E, with a total area of 1.2 × 10^6 km^2 and a population of 123,379,924 in 2022. The country's topography has highly contrasting features, with varying altitudes, highland complexes of mountains to the north, lowland to the east, with the Great East African Rift Valley in the south. Figure 1 shows the 12 river basins of Ethiopia, such as the Rift Valley, Omo-Ghibe, Baro-Akobo, Abbay, Tekeze, Mereb, Afar/Denakil, Awash, Aysha, Ogaden, Wabi-Shebelle, and Genale Dawa. The country is characterized by high temporal and spatial climatic variability. There are three different rainfall seasons in the country: the main rain season ranges from June to September, the dry season ranges from October to January, and the short rain season ranges from February to May, but the southern and southeastern parts of the country have bilateral rainfall distribution, with rain falling from March to May and from September to November. Due to different weather systems, there is high spatiotemporal variation of rainfall in each river basin (Gebere *et al.* 2015; Bayissa *et al.* 2017; Lemma *et al.* 2022).

2.2. Data collection

There are different satellite data products that are useful for the estimation of the water budget, such as combined Tropical Rainfall Measuring Mission (TRMM) and Global Precipitation Measurement (GPM) precipitation, which was Integrated Multi-Satellite Retrievals for GPM (MERG) as spatial and temporal resolution product at 0.1° × 0.1°, Terra and Aqua MODIS at 500 m, liquid water equivalent thickness from GRACE data product at 1° × 1°, GLDAS data product at 0.25° × 0.25°, Terra-Climate, and others. But, for this study, GRACE and GLDAS data products were used to estimate the long-term water storage of major river basins of Ethiopia. All-important data were collected to accomplish this research and discussed as follows.

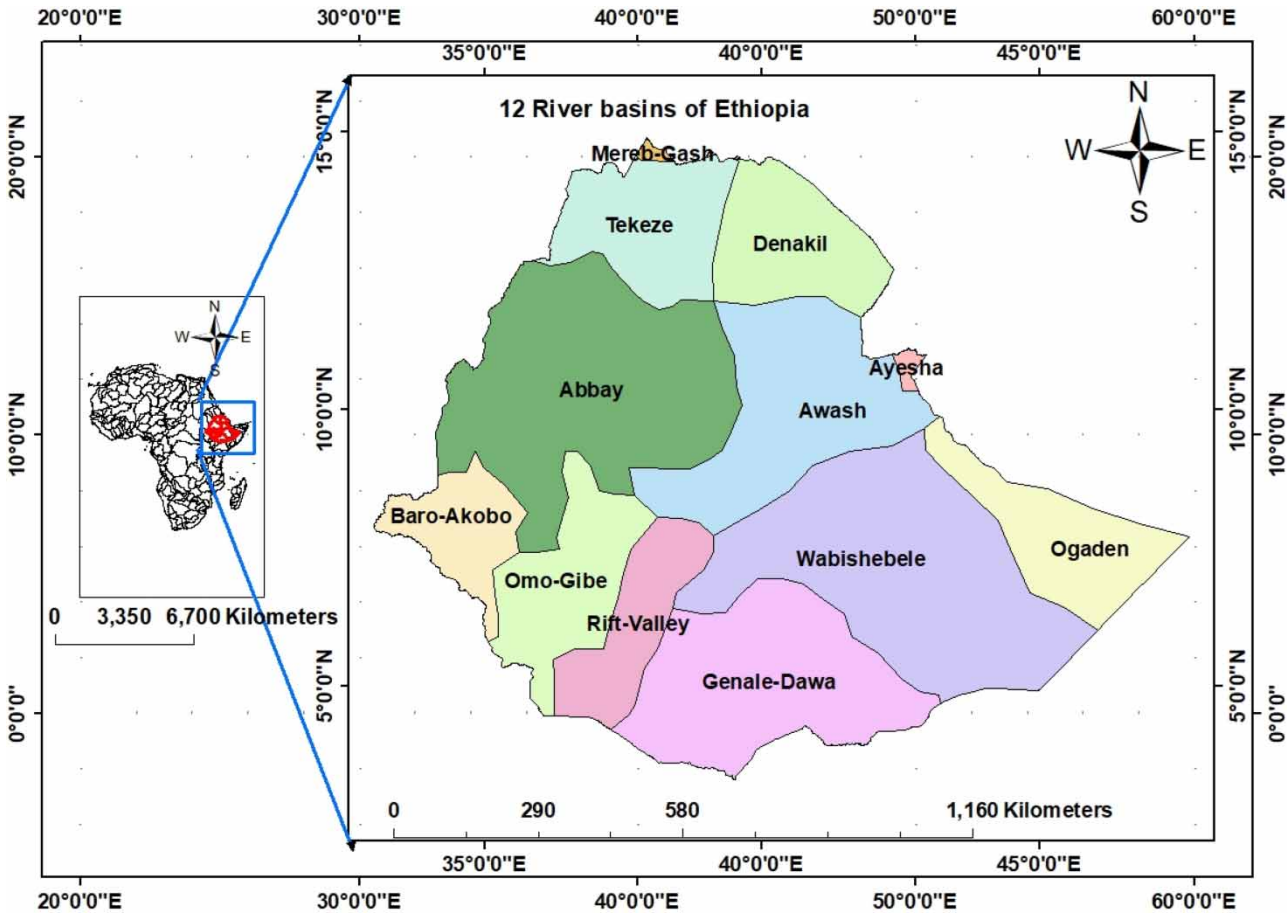

Figure. 1 | Location map of the study area for the major river basins of Ethiopia.

2.3. Methods for data analysis

2.3.1. Equivalent water thickness by the GRACE satellite

The Mascon method directly estimates the liquid equivalent water thickness based on the mass change in a certain region, mainly through high-precision inter-satellite observation of data from the GRACE satellites. Its surprising feature is that the earth mass change is directly estimated as a parameter, and thus, it is more flexible with respect to the region of interest (Swenson & Wahr 2002; Wang *et al.* 2019). Watkins *et al.* (2015) designed 4,551 spherical caps of equal area with uniform mass distribution (Mascon) on a global scale and estimated the liquid equivalent water thickness of each ball cap through the weighted least squares method, using the three GRACE satellite datasets. During satellite data tracing, there was signal loss, which had to be removed to find the gravitational anomaly coefficient, and then, the spherical harmonic coefficient was obtained by the band limit of Stokes coefficient at spherical harmonic degree (Wahr *et al.* 1998). The damping of the signal amplitude due to filtering causes leakages (Vishwakarma *et al*. 2017; Chen *et al*. 2019; Koster & Suarez 2022) have undergone pre-processing, such as de-striping filter, Gaussian smoothing, and glacier isostatic adjustment (Chen *et al*. 2019). The accuracy of the GRACE product was improved by averaging the three datasets (Landerer & Swenson 2012; Seyoum & Milewski 2017), and the missing data were filled by linear interpolation (Long *et al.* 2015). To restore the original signal that was lost during data processing, a multiplicative scaling factor was used for the monthly data provided by the GRACE product (Seyoum *et al.* 2019), and more information about scaling factors can be found in Landerer & Swenson (2012). In this study, the spatiotemporal distribution of the three datasets were collected for each river basin.

2.3.2. Global Land Data Assimilation System

GLDAS is a commonly used land surface modeling, with the objective of producing an optimal field of land surface states and fluxes based on satellite and ground observations, and has been frequently used for the calculation of terrestrial water storage and groundwater storage (Rodell *et al.* 2004; Syed *et al.* 2008; Nie *et al.* 2016; Hsu *et al.* 2020). Four land surface models (LSMs) were used by GLDAS to provide hydrological data of the area, such as the variable infiltration capacity (VIC) (Liang *et al.* 1998), the community land model (CLM) (Dai *et al.* 2013), Mosaic (Koster & Suarez 2022), and Noah (Ek *et al.* 2003). The average of the four LSMs datasets (VIC, Noah, CLM, and Mosaic) was utilized to estimate the anomaly of SWE, SM, and CWS to reduce any errors or biases (Katpatal *et al.* 2018). For the estimation of the change in terrestrial water storage from GLDAS, 22 bands were utilized with $1° \times 1°$ spatial resolution (Li *et al.* 2019). The validation of GLDAS result is confirmed by water resources and climate studies in Iran, where lack of observations inhibits advanced hydro climatological studies and sustainable water resource management (Moghim 2018). In this study, spatiotemporal variations of the GLDAS dataset were collected for each river basin.

2.3.3. Climatic dataset

During this study, climatic datasets like precipitation, temperature, and others were collected from the power project data products, which is the Prediction of Worldwide Energy Resources (POWER) Project, which provides solar and meteorological data from NASA research for support of renewable energy, building energy efficiency, and agricultural needs. In this data product, there are multiple data access options using the Data Access Viewer, which is a responsive web mapping application that provides data subsetting, charting, and visualization tools in an easy way.

2.3.4. Data of human activities

The grazing data, mining data, agricultural data, and other human activities in each river basin were collected from ministry of water and Energy of Ethiopia (https://www.mowe.gov.et). In addition, detailed information about human activities in each river basin was collected from the regional water and energy offices during study durations.

2.3.5. Water storage equation

For each river basin, major water budget components were collected, and changes in terrestrial water storage are estimated in Equation (1):

$$\Delta TWS = \Delta GWS + \Delta SWS + \Delta SMS + \Delta CWS + \Delta SNWS \quad (1)$$

where ΔTWS is a change in terrestrial water storage, ΔGWS is a change in groundwater storage, ΔSMS is a change in soil moisture storage, ΔSNWS is a change in snow water storage, and ΔCWS is change in canopy water storage. For each river basin, ΔSNWS was neglected, because the area does not experience snow water storage due to the climatic condition of Ethiopia.

2.3.6. Water balance equation

Evapotranspiration and precipitation are a key component of both atmospheric and terrestrial water storage (Meng *et al.* 2019). The precipitation minus evapotranspiration shows the net water flux on to the earth's surface and gives essential information regarding the interaction between the atmosphere and the land surface (Swenson & Wahr 2006). For each river basin, the relationship between terrestrial water, precipitation, and evapotranspiration can be expressed as in Equation (2):

$$\Delta \mathrm{LWE} = \mathrm{RF} - \mathrm{EVT} \tag{2}$$

EVT is affected by both natural climate factors and anthropogenic factors such as irrigation or groundwater pumping (Pan *et al.* 2017). But GLDAS only simulates EVT under natural climate conditions. RF-EVT obtained from GLDAS was compared with terrestrial water storage (TWS) from GRACE, the former of which reflects TWS changes under natural climate conditions and the latter represents the total TWS change, to evaluate the contribution of human activities to TWS changes. Moreover, to estimate the effects of human activities on the variations in EVT, EVT calculated from GLDAS was compared with the total EVT obtained from GRACE. The total EVT can be estimated by Equation (3):

$$\mathrm{EVT}_{\mathrm{GRACE}} = \mathrm{RF} - \mathrm{LWE}_{\mathrm{GRACE}} \tag{3}$$

where $\mathrm{EVT}_{\mathrm{GRACE}}$ shows total EVT and $\mathrm{LWE}_{\mathrm{GRACE}}$ is liquid water equivalent obtained from GRACE.

2.3.7. Reconstruction of climate-driven water storage anomalies

We reconstructed the climatic water storage anomalies in the major river basins of Ethiopia based on GRACE and GLDAS datasets, precipitation and temperature data by using data-driven statistical methods proposed by Humphrey ($\mathrm{CWSA}_{\mathrm{Humphrey}}$) (Humphrey & Gudmundsson 2019; Humphrey *et al.* 2017). $\mathrm{CWSA}_{\mathrm{Humphrey}}$ is calculated as follows:

$$\mathrm{TWSA}_{\mathrm{REC}} = \beta_1 * P^{\tau}_{\mathrm{inter+subseas}} + \beta_2 * T_{\mathrm{inter}} + \varepsilon \tag{4}$$

$$\mathrm{TWSA}_{\mathrm{Humphrey}} = \mathrm{TWSA}_{\mathrm{REC}} + \mathrm{TWSA}_{\mathrm{seasonal}} \tag{5}$$

where $\mathrm{TWSA}_{\mathrm{REC}}$ is the reconstructed terrestrial water storage anomalies without the trend and seasonal signals, and $P^{\tau}_{\mathrm{inter+subseas}}$ is the de-seasonal and de-trended precipitation data. The decay parameter τ controls the steepness of the exponential decay filter applied to the daily precipitation time series before averaging to the monthly resolution. T_{inter} corresponds to the monthly interannual temperature, parameters β_1 and β_2 correspond to calibrated scaling coefficients, ε is an error term, and $\mathrm{TWSA}_{\mathrm{seasonal}}$ represents the GLDAS- and GRACE-based seasonal cycle of water storage variation.

2.3.8. Independent component analysis

To better illustrate the change in complex hydrological signals, ICA was used to identify the main spatiotemporal characteristics of GRACE and GLDAS terrestrial water storage. Let m unknown source of signals that forms column vector, $S_t = [S_1(t_1),\ S_2(t_2) \ldots\ldots\ S_n(t_n)]^T$, and A is an unknown mixing matrix representing the spatial distribution of the source signals (Hyvarinen 1999; Bingham & Hyvärinen 2000; Hyvarinen & Oja 2000). Assuming n observation channels for each river basin, the ICA can be formulated as follows:

$$\begin{bmatrix} x_1(t_1) & \cdots & x_1(t_m) \\ \vdots & \ddots & \vdots \\ x_n(t_1) & \cdots & x_n(t_m) \end{bmatrix} = A \begin{bmatrix} S_1(t_1) & \cdots & S_1(t_m) \\ \vdots & \ddots & \vdots \\ S_n(t_1) & \cdots & S_n(t_m) \end{bmatrix} = AS(t) \tag{6}$$

The objective of ICA is to evaluate both the source of signals $S(t)$ and the mixing matrix A from the observed data $X(t)$. ICA makes use of statistical independence as a criterion for separating the source signals. The idea of ICA is to set up linear

decomposition matrix W, where X is transferred by W to obtain an n-dimensional random variable sequence $Y(t) = [y_1(t),\ y_2(t),\ \ldots . y_n(t)]^T$:

$$Y(t) = WX(t) = WDS(t) \tag{7}$$

ICA obtains the source signals by optimizing the decomposition matrix W so that the independence between the source signals is strongest. When the best decomposition matrix W is determined, the mathematically defined $Y(t)$ are referred to as independent components (ICs). In this study, ICA can be used to separate the source signals of terrestrial water storage. By comparing the source signals of the terrestrial water storage with the other hydrological products, it is possible to quantify the contributions of different drive factors to the variations in the terrestrial water storage anomalies over the study period.

2.3.9. Correlation analysis

To estimate the consistency and similarity of terrestrial water storage from GLDAS and GRACE, Pearson's correlation coefficient was used, as shown in Equation (4):

$$r(\mathrm{GR}, \mathrm{GL}) = \frac{\sum_{i=1}^{n} (\mathrm{GR}_i - \bar{\mathrm{GR}})(\mathrm{GL}_i - \bar{\mathrm{GL}})}{\sqrt{\sum_{i=1}^{n} (\mathrm{GR} - \bar{\mathrm{GR}})^2} \sqrt{\sum_{i=1}^{n} (\mathrm{GL} - \bar{\mathrm{GL}})^2}} \tag{8}$$

where GR is the monthly terrestrial water storage estimated from GLDAS, GL is the monthly/hydro climatic factors calculated from GLDAS, and n is the number of months.

2.3.10. Evaluation of methods of model performance

To calculate the downscaled terrestrial water storage results, four different statistical metrics were used, including mean absolute error (MAE), Nash–Sutcliffe efficiency (NSE), Pearson's correlation coefficient (R), and root-mean-square error (RMSE). The mathematical representation of MAE, NSE, R, and RMSE is shown in Equations (7)–(10). For RMSE and MAE, the values close to 0 indicate the perfect model, whereas in NSE and R, the value closer to 1 indicates the perfect model:

$$\mathrm{RMSE} = \sqrt{\frac{\sum_{i=1}^{N} (X_i - Y_i)^2}{N}} \tag{9}$$

$$\mathrm{NSE} = 1 - \frac{\sum_{i=1}^{N} (Y_i - \bar{Y})^2}{\sum_{i=1}^{N} (X_i - \bar{X})^2} \tag{10}$$

$$R = \frac{\sum_{i=1}^{N} (X_i - \bar{X})(Y_i - \bar{Y})}{\sqrt{\sum_{i=1}^{N} (X_i - \bar{X})^2} \sqrt{\sum_{i=1}^{N} (Y_i - \bar{Y})^2}} \tag{11}$$

$$\mathrm{MAE} = \frac{1}{N} \left(\sum_{i=1}^{N} |Y_i - X_i| \right) \tag{12}$$

where X_i and Y_i indicate two independent datasets with the mean value of X and Y. The input terrestrial water storage is represented by X_i, and the predicted value of random forest model is represented by Y_i. N represents the total number of samples. Figure 2 indicates the generalized methodology of the study area.

3. RESULTS AND DISCUSSION

3.1. Liquid water equivalent thickness from GRACE over the major river basins of Ethiopia

In this study, GRACE liquid water equivalent thickness was evaluated from three different sources (CSR, JPL, and GFZ) for Ethiopia's river basins based on the dataset from 2002 to 20016. We estimated a multiplicative scale factor of 1.04 using Gaussian smoothing to restore the original signal lost during data processing. All the missing data for each river basin were

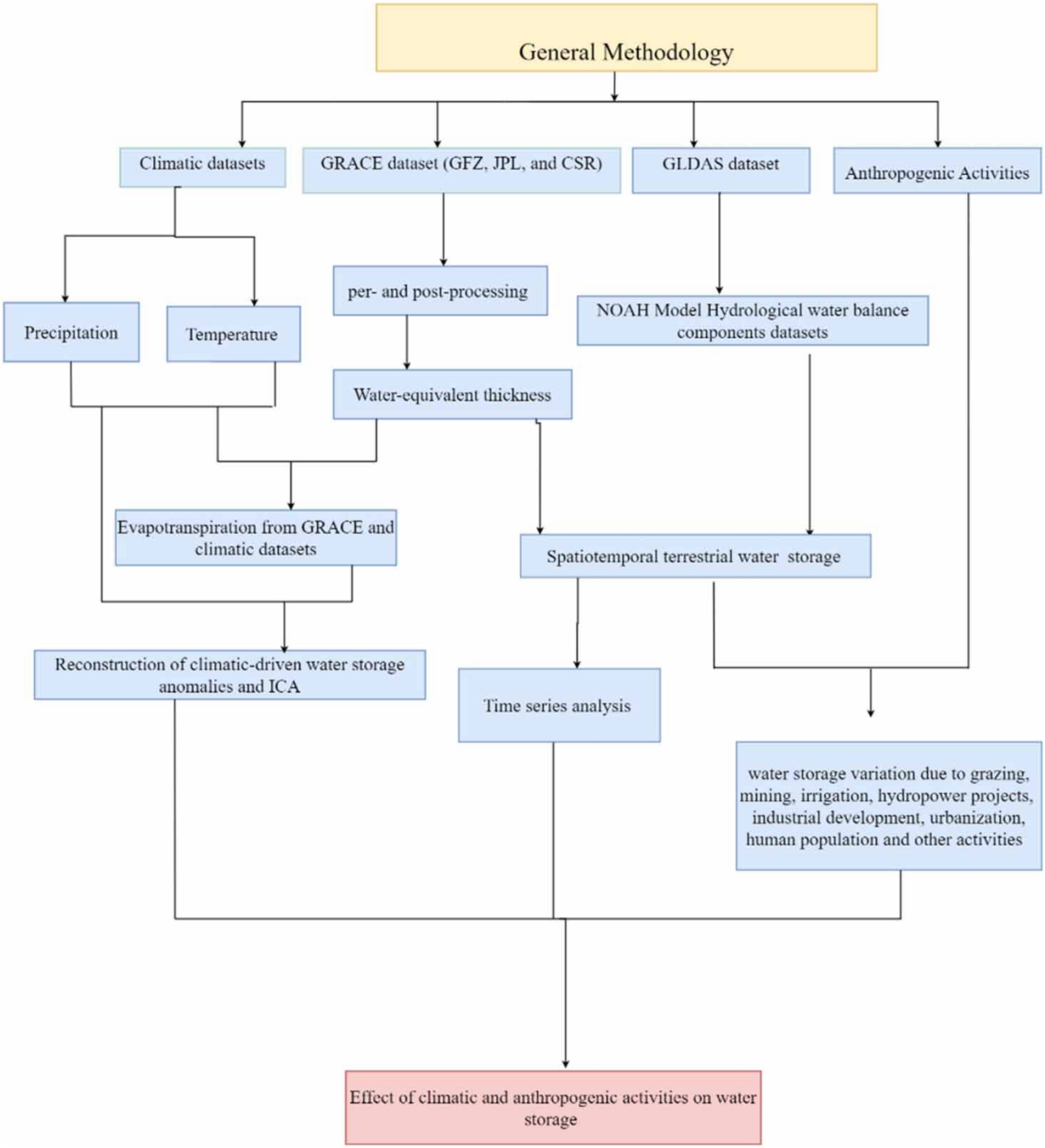

Figure 2 | The generalized methodology of the study area.

calculated using linear interpolation and the average result for each river basin is shown in Figure 3. Temporal characteristics of the three datasets for each river basin were evaluated and additionally, cross-correlation between the three data products (CSR + JPL, CSR + GFZ, and GFZ + JPL) were evaluated for each river basin, and the result indicates a significant correlation coefficient of Abbay (0.97, 0.96, and 0.95), Awash (0.95, 0.91, 0.93), Ayesha (0.9, 0.83, 0.87), Baro-Akobo (0.98, 0.97, 0.96), Denakil (0.9, 0.83, 0.85), Genale Dawa (0,91, 0.88, 0.9), Mereb Gash (0.86, 0.76, 0.8), Ogaden (0.85, 0.71, 0.73), Omo-Gibe (0.96, 0.95, 0.94), Rift Valley (0.94, 0.92, 0.91), Tekeze (0.93, 0.88, 0.9), and Wabishebele River Basin

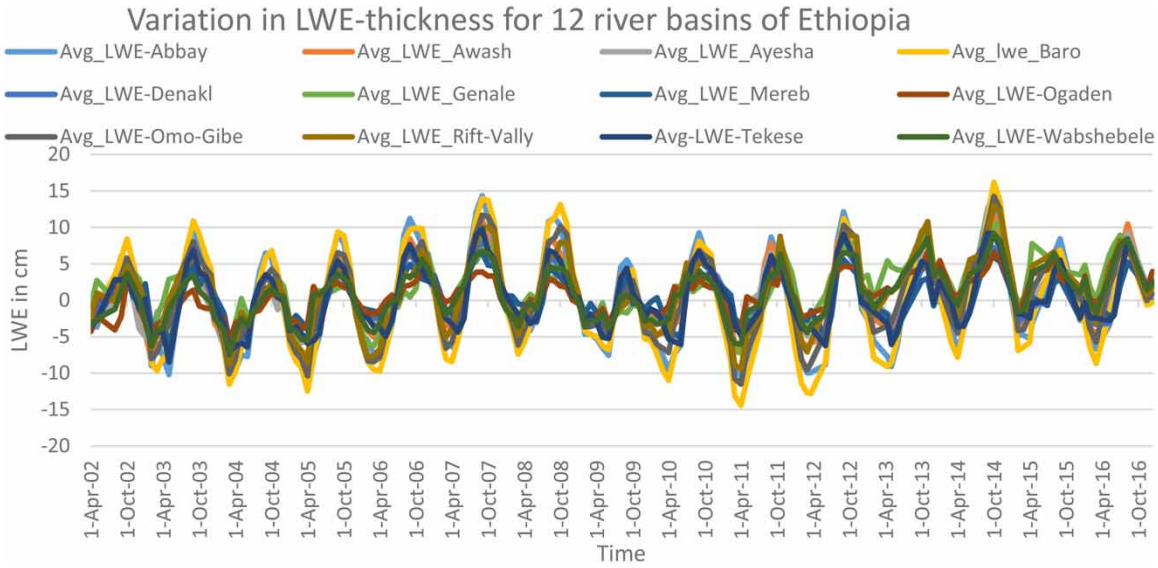

Figure 3 | Characteristic of average LWE for the major river basins of Ethiopia.

(0.9, 0.84, 0.87), respectively. In addition, for each river basin, liquid water equivalent thickness reach a minimum and maximum simultaneously. Figure 5 displays mean annual variation of LWE over major river basins of Ethiopia from 2002 to 2016, averaged from the three GRACE-driven datasets. Liquid water equivalent thickness from GRACE (LWE) is estimated as the average of the three-derived datasets with the view of diminishing the noise of the LWE thickness. The mean monthly LWE observed for Abbay basin ranges from −10.43 to 14.68 cm/month, Awash (−9.19 to 11.6 cm/month), Ayesha (−7.44 to 9.32 cm/month), Baro-Akobo (−14.4 to 16.2 cm/month), Denakil (−7.59 to 7.93 cm/month), Genale Dawa (−7.22 to 10.74 cm/month), Mereb Gash (−6.2 to 6.57 cm/month), Ogaden (−5.84 to 7.08 cm/month), Omo-Gibe (−11.49 to 14.25 cm/month), Rift Valley (−9.4 to 12.24 cm/month), Tekeze (−8.47 to 9.81 cm/month), and Wabishebele River Basin (−7.54 to 9.17 cm/month). Specifically, the LWE variation shows a distinct seasonal cycle. The maximum and minimum value of LWE for Abbay river basin was observed in September and April, Awash (September and March), Ayesha (September and February), Baro (October and March), Denakil (September and April), Genale Dawa (November and March), Mereb Gash (September and May), Ogaden (November and March), Omo-Gibe (October and March), Rift Valley (October and March), Tekeze (September and May), and Wabishebele (October and March). Generally, this section reports that the terrestrial water storage derived from GRACE shows both the potential for revealing variation in terrestrial water storage and the ability to support hydrological modeling, which agrees with previous findings conducted in many river basins (Li *et al.* 2013, 2018; Ni *et al.* 2014; Feng *et al.* 2017; khaki *et al.* 2018; Wang *et al*. 2019).

3.1.1. Spatial distribution of liquid water equivalent thickness from GRACE

To understand the spatial distribution of GRACE LWE for the major river basins of Ethiopia, we next performed a grid-to-grid process to obtain the long-term trend, which is defined as the monthly average rate of the terrestrial water storage change. As presented in Figure 4, overall, the spatial distributions of the LWE trend over the major river basins of Ethiopia retrieved by GRACE from April 2002 to January 2017, was averaged for different seasons. For each river basin, the LWE shows obvious seasonal variation from spring to winter for all river basins, and we observe spatial variation of LWE for Abbay (−2.07 to 0.68 cm/month), Tekeze (−0.44 to 1.04 cm/month), Mereb Gash (−0.44 to 0.47 cm/month), Denakil (−0.82 to 1.04 cm/month), Awash (−0.41 to 1.85 cm/month), Ayesha (1.46 cm/month), Baro-Akobo (−2.1 to 2.43 cm/month), Omo-Gibe (−1.42 to 4.41 cm/month), Rift Valley (0.82 to 4.89 cm/month), Genale Dawa (2.78 to 5.6 cm/month), Wabishebele (0.69 to 3.57 cm/month), and Ogaden (1.45 to 2.11 cm/month). Abby River Basin (Figure 4(1)) experiences high LWE in northern and eastern parts of the river basin and low LWE in southwestern parts of the river basin; Tekeze River Basin experiences low LWE in north eastern parts and high LWE in western parts of the river basin (Figure 4(2)); Mereb Gash experiences high LWE in western parts and low LWE in eastern parts of the river basin (Figure 4(3)); Denakil experiences increasing LWE

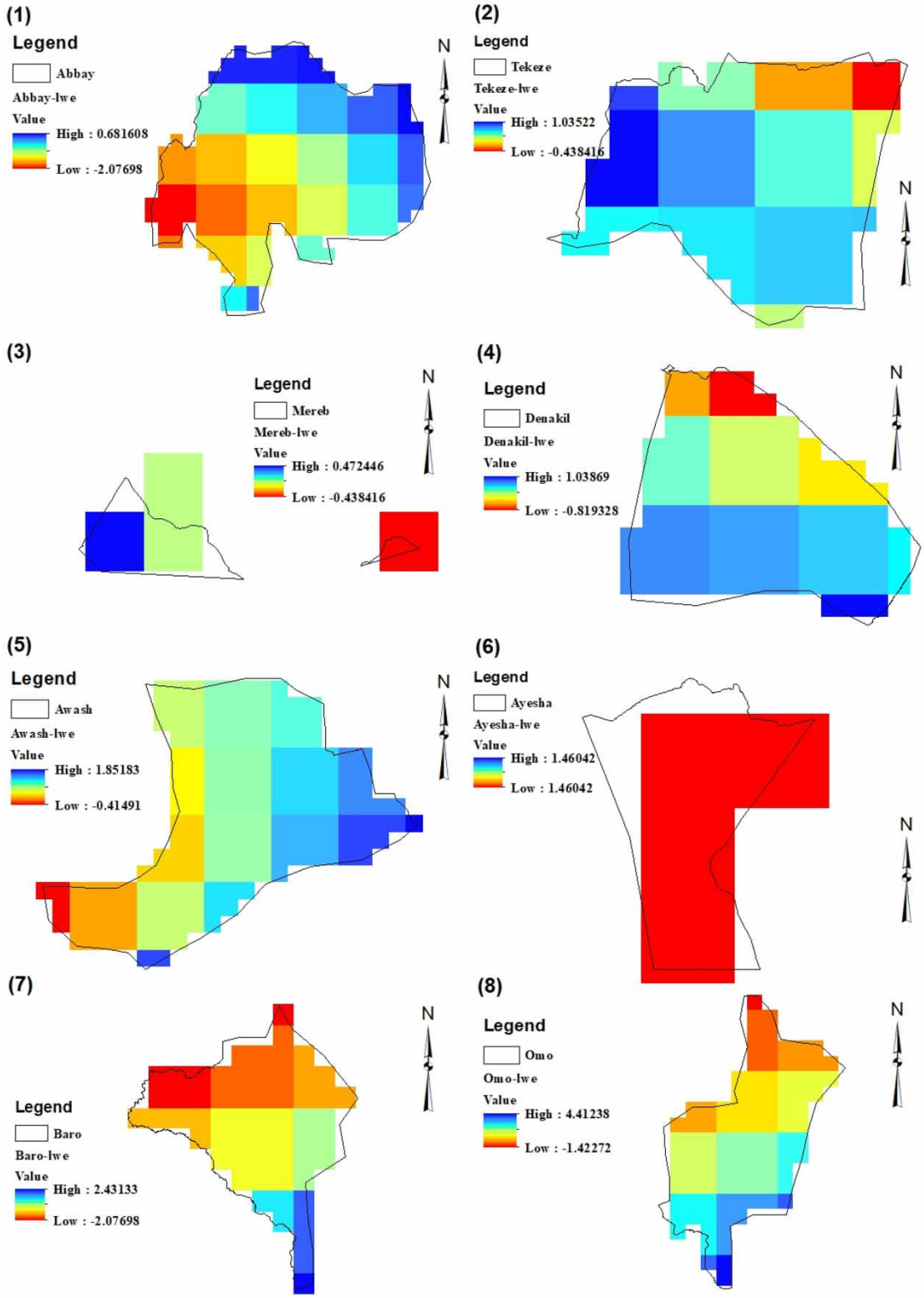

Figure 4 | Spatial variation of average LWE from GRACE for the 12 river basins of Ethiopia from 2002 to 2016. (1) Spatial distribution of LWE for Abbay, (2) spatial distribution of LWE for Tekeze, (3) spatial distribution of LWE for Mereb Gash, (4) spatial distribution of LWE for Denakil, (5) spatial distribution of LWE for Awash, (6) spatial distribution of LWE for Aysha, (7) spatial distribution of LWE for Baro-Akobo, (8) spatial distribution of LWE for Omo-Gibe, (9) spatial distribution of LWE for Rift Valley, (10) spatial distribution of LWE for Genale Dawa, (11) spatial distribution of LWE for Wabishebel, and (12) spatial distribution of LWE for Ogaden. (*continued*.).

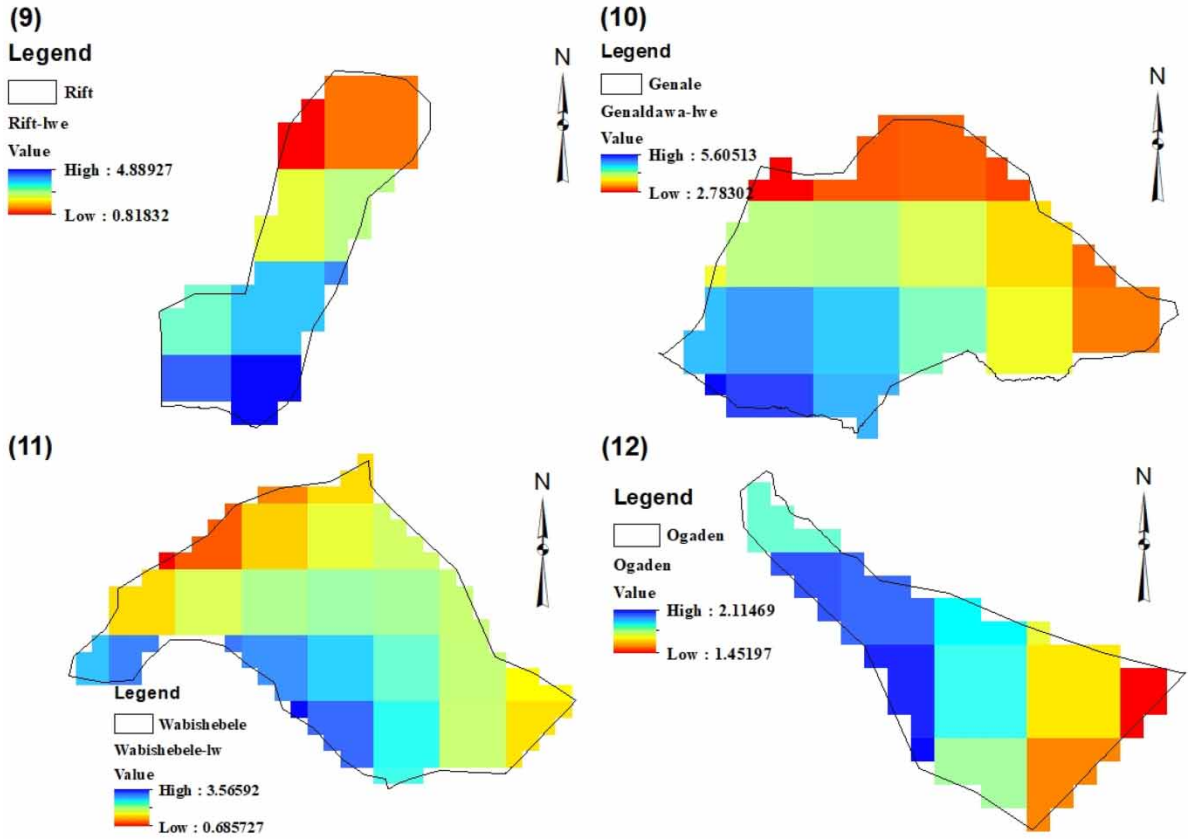

Figure 4 | Continued.

over the basin from north to southern parts of the river basin (Figure 4(4)); Awash experiences decreasing LWE from eastern to southwestern parts of the river basin(Figure 4(5)); Ayesha experiences low LWE (Figure 4(6)); Baro-Akobo (Figure 4(7)), Omo-Gibe (Figure 4(8)), Rift Valley (Figure 4(9)), and Genale Dawa (Figure 4(10)) experiences the increasing LWE from south to northern parts of the river basin; Wabishebele experiences the increasing LWE from north to south (Figure 4(11)); and Ogaden experiences decreasing LWE from western to eastern parts of the river basin (Figure 4(12)). The spatial variation of the terrestrial water storage was largely related to the topographic variation of each river basin.

3.1.2. Estimation of temporal variation of liquid water equivalent thickness from GRACE

Figure 5 displays mean annual variation of LWE over major river basins of Ethiopia from 2002 to 2016, averaged from the three GRACE-driven datasets. Based on the estimated result, minimum and maximum range of LWE are as follows: Ayesha, −26.85 to 39.68 cm/year (Figure 5(1)); Awash, −29.75 to 41.01 cm/year (Figure 5(2)); Denakil, −20.21 to 25.07 cm/year (Figure 5(3)); Baro-Akobo, −46.9 to 33.4 cm/year (Figure 5(4)), Genale Dawa, −20.62 to 57.36 cm/year (Figure 5(5)); Mereb Gash, −16.95 to 23.83 cm/year (Figure 5(6)); Ogaden, −24.73 to 6.5739.29 cm/year (Figure 5(7)); Omo-Gibe, −22.58 to 50.20 cm/year (Figure 5(8)); Rift Valley, −20.03 to 60.05 cm/year (Figure 5(9)); Tekeze, −20.81 to 30.42 cm/year (Figure 5(10)); Wabishebele, −22.75 to 47.32 cm/year (Figure 5(11)); and Abbay River Basin −28.58 to 34.21 cm/year, respectively. The lowest LWE for each river basin was observed in 2004 for Ayesha, Awash, Denakil, Mereb Gash, Omo-Gibe, Tekeze, Wabishebele, and Abbay; in 2011 for Baro-Akobo, in 2009 for Genale Dawa, in 2003 for Rift Valley; and in 2002 for Ogaden River Basin. Generally, the estimated mean annual LWE observed for each river basin shows high fluctuation of LWE. The fluctuation of the LWE for all river basins were observed in 2002, 2003, 2004, 2007, 2009, 2010, 2011, 2013, and 2014, and this is in good agreement with drought occurrence findings in Ethiopia for all river basins (Edossa *et al.* 2010; Bayissa *et al.* 2015; Yisehak *et al.* 2021). Many studies also confirm that severe drought has

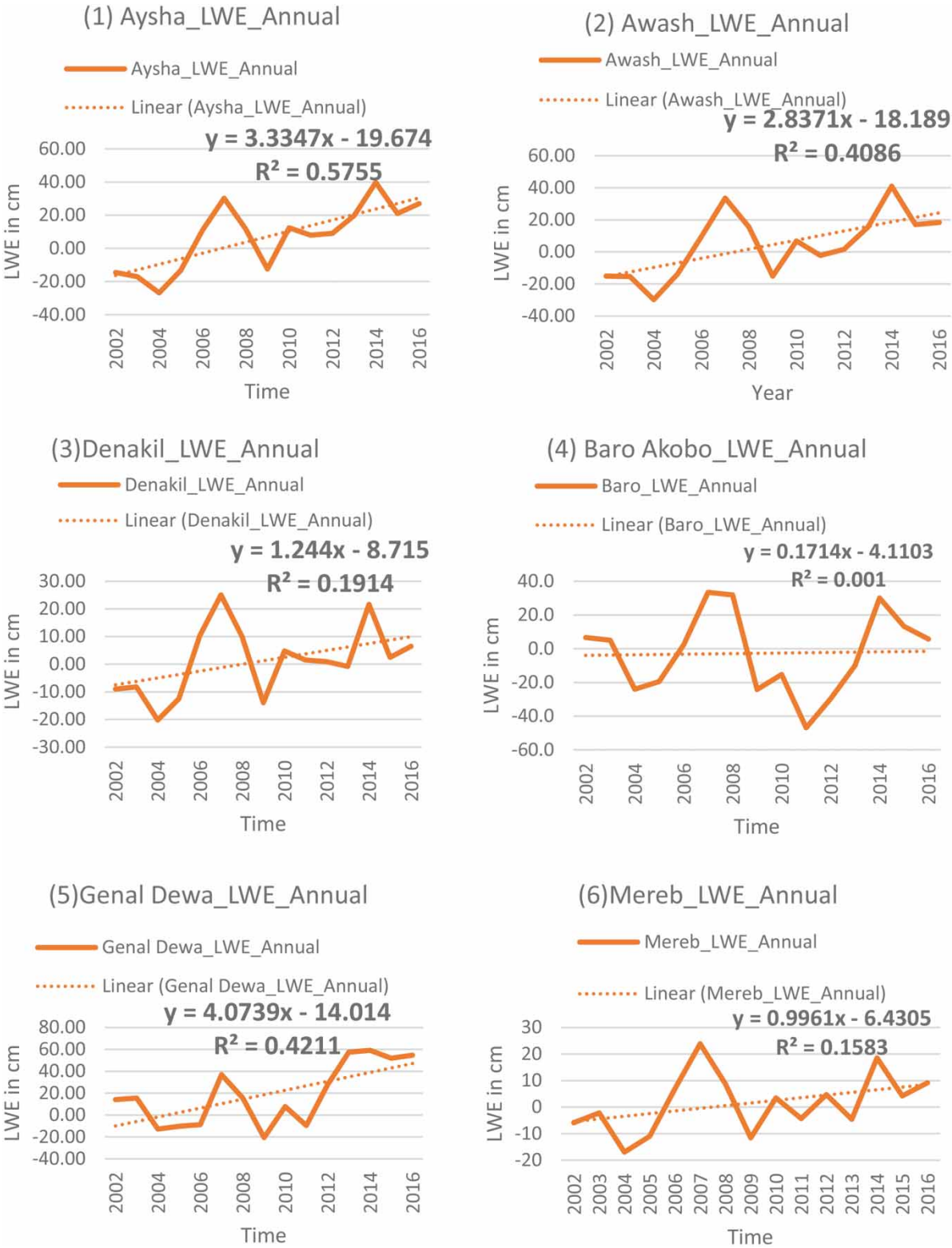

Figure 5 | Temporal variation of mean annual LWE from GRACE for the major river basins of Ethiopia from 2002 to 2016. (1) Temporal variation of LWE for Ayesha, (2) temporal variation of LWE for Awash, (3) temporal variation of LWE for Denakil, (4) temporal variation of LWE for Baro-Akobo, (5) temporal variation of LWE for Genale Dawa, (6) temporal variation of LWE for Mereb Gash, (7) temporal variation of LWE for Ogaden, (8) temporal variation of LWE for Omo-Gibe, (9) temporal variation of LWE for Rift Valley, (10) temporal variation of LWE for Tekeze, (11) temporal variation of LWE for Wabishebel, and (12) temporal variation of LWE for Abbay. (*continued.*).

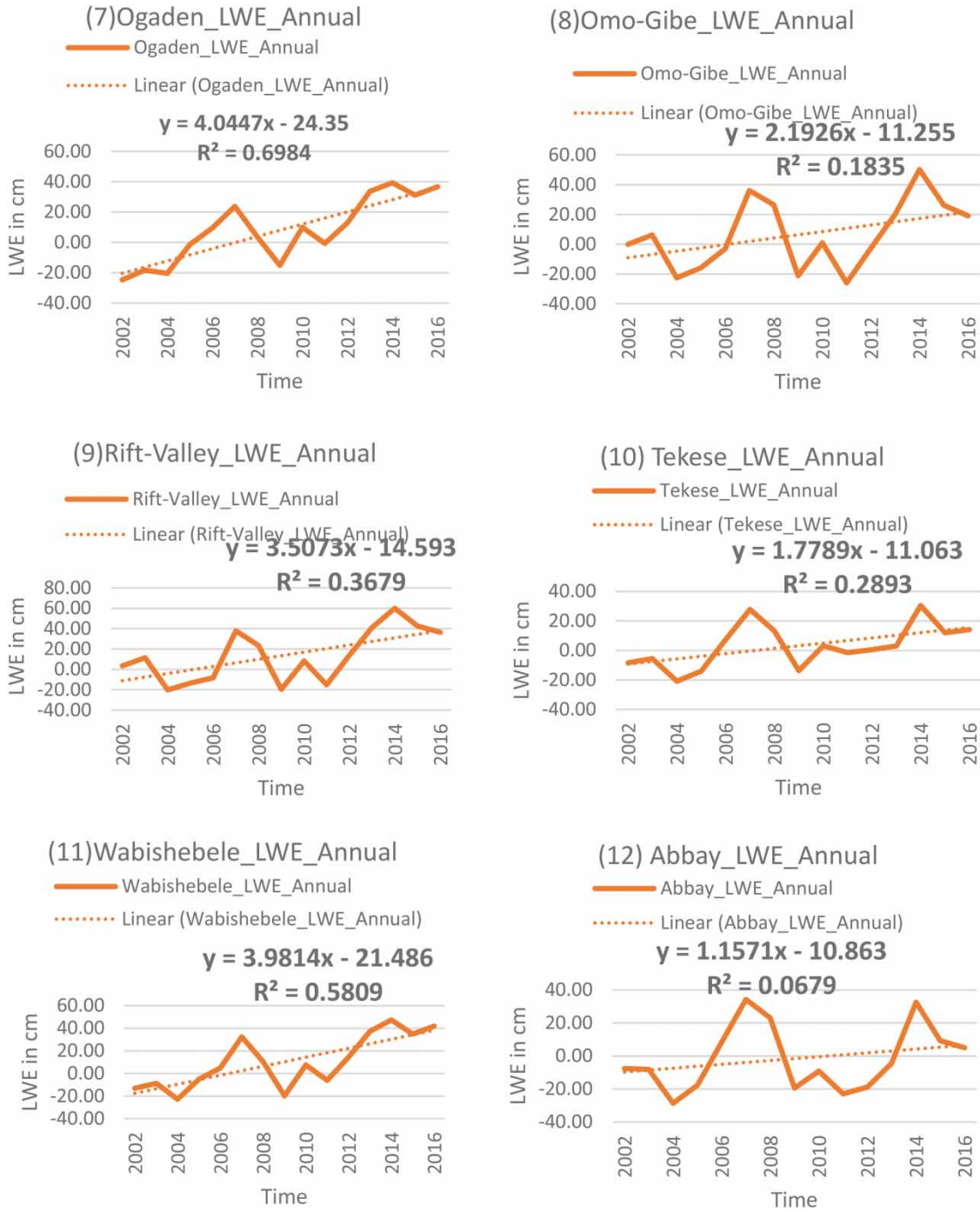

Figure 5 | Continued.

occurred in these years and caused substantial damage in terms of life and economic loss (Edossa *et al.* 2010; Gebrehiwot *et al.* 2011; Bayissa *et al.* 2015; Gidey *et al.* 2018; Seyoum *et al.* 2019; Yisehak *et al.* 2021).

3.2. Estimation of terrestrial water storage changes over the major river basins of Ethiopia from GLDAS

Terrestrial water storage calculated from GLDAS includes soil moisture, plant canopy water storage, ground water storage, and snow water storage, which account for the total water balance of any area (Chao *et al.* 2018). Furthermore, from the perspective of the water cycle, the change in terrestrial water storage can also be denoted by changes in precipitation,

evapotranspiration, and runoff (Wang *et al.* 2007; Thompson *et al.* 2011; Yang *et al.* 2017). For each river basin, the snow water storage was neglected, and the terrestrial water storage for each river basin was quantified from GLDAS data products from 2010 to 2020 in this section by using Equation (1), and the result of variation in terrestrial water storage and year-to-year vitiations for the major river basins of Ethiopia are presented in Figure 6, which demonstrates a distinct seasonal cycle. The temporal series shows simultaneous falling and rising, which coincides with a steady decline (dry period) and peak amplitude (wet period) during the study period. The characteristics of the change in the trend were consistent with the overall change in terrestrial water storage, indicating that the change in terrestrial water storage mainly depends on trend terms. The terrestrial water storage reflects high fluctuations and was the most powerful evidence for drought or flood events in each river basin. The mean monthly estimated GLDAS TWS for Abbay river basin from 36,458.2–53,766.74 mm/month, Awash (22,077.49–30,655.13 mm/month), Ayesha (15,263.46–19,443.88 mm/month), Baro-Akobo (37,337.18–49,829.36 mm/month), Denakil (17,445.87–22,088.63 mm/month), Genale Dawa (22,308.8–32,241.64 mm/month), Mereb Gash (24,451.09–33,359.96 m/month), Ogaden (20,574.79–27,144.18 mm/month), Omo-Gibe (34,832.42–51,615.8 mm/month), Rift Valley (25,871.97–42,016.34 mm/month), Tekeze (25,552.41–35,765.87 mm/month), and Wabishebele River Basin (22,302.61–30,237.48 mm/month). The lowest GLDAS TWS for all river basins were observed in February, whereas the highest GLDAS TWS for Abbay (October), Awash (September), Ayesha (December), Baro (October), Denakil (August), Genale Dawa (May), Mereb Gash (September), Ogaden (May), Omo-Gibe (October), Rift Valley (October), Tekeze (September), and Wabishebele (December). The highest GLDAS TWS was observed for Abbay, Omo-Gibe, and Baro-Akobo, whereas the lowest GLDAS TWS was observed in the Ayesha, Denakil, Ogaden River Basin, and the other river basins have medium TWS (Figure 6). This study agrees with the previous studies (Syed *et al.* 2008; Thompson *et al.* 2011; Luo *et al.* 2016; Nie *et al.* 2016; Yang *et al.* 2017).

3.2.1. Yearly and seasonal variation of GLDAS terrestrial water storage for the major river basins of Ethiopia

Figure 7(1–12) indicates the annual trends of terrestrial water storage for the study area from 2010 to 2020. Looking at individual river basins, the variation in terrestrial water storage was affected by seasonal variations, maximum terrestrial water storage was observed during spring and summer in the Ogaden and Ayesha River Basin; during Autumn in Abbay,

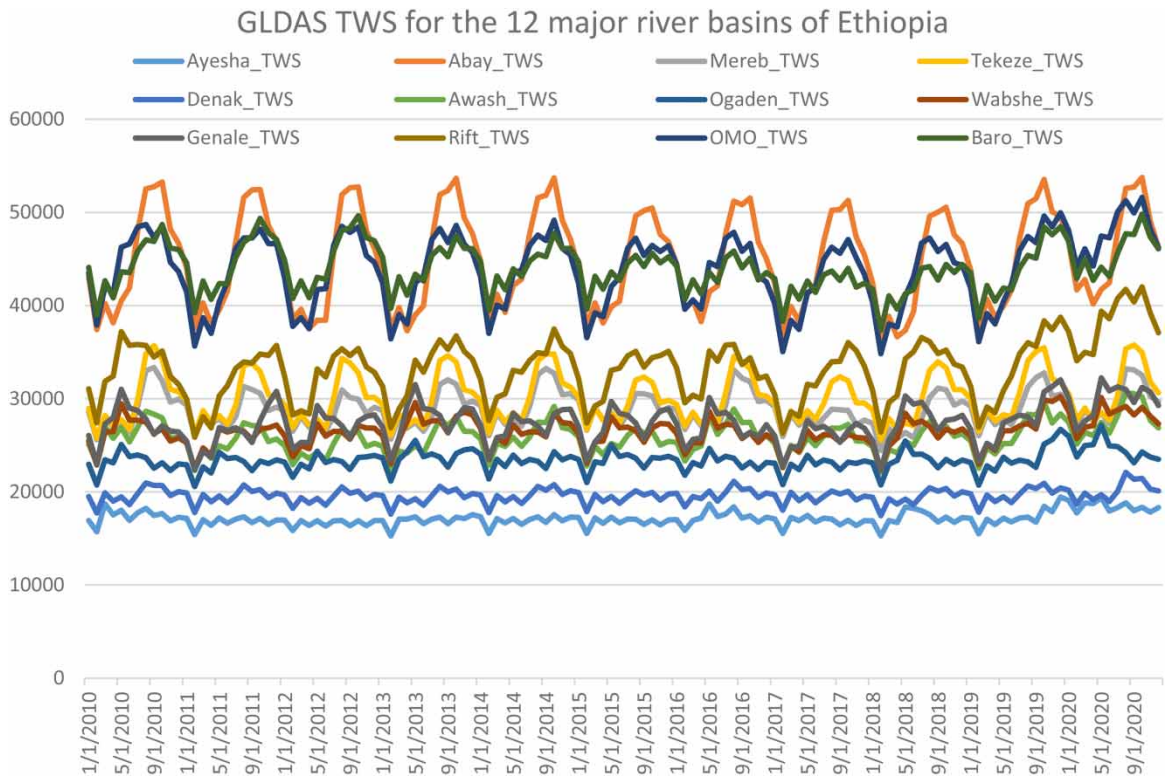

Figure 6 | Terrestrial water storage estimated from GLDAS data products for the major river basins of Ethiopia.

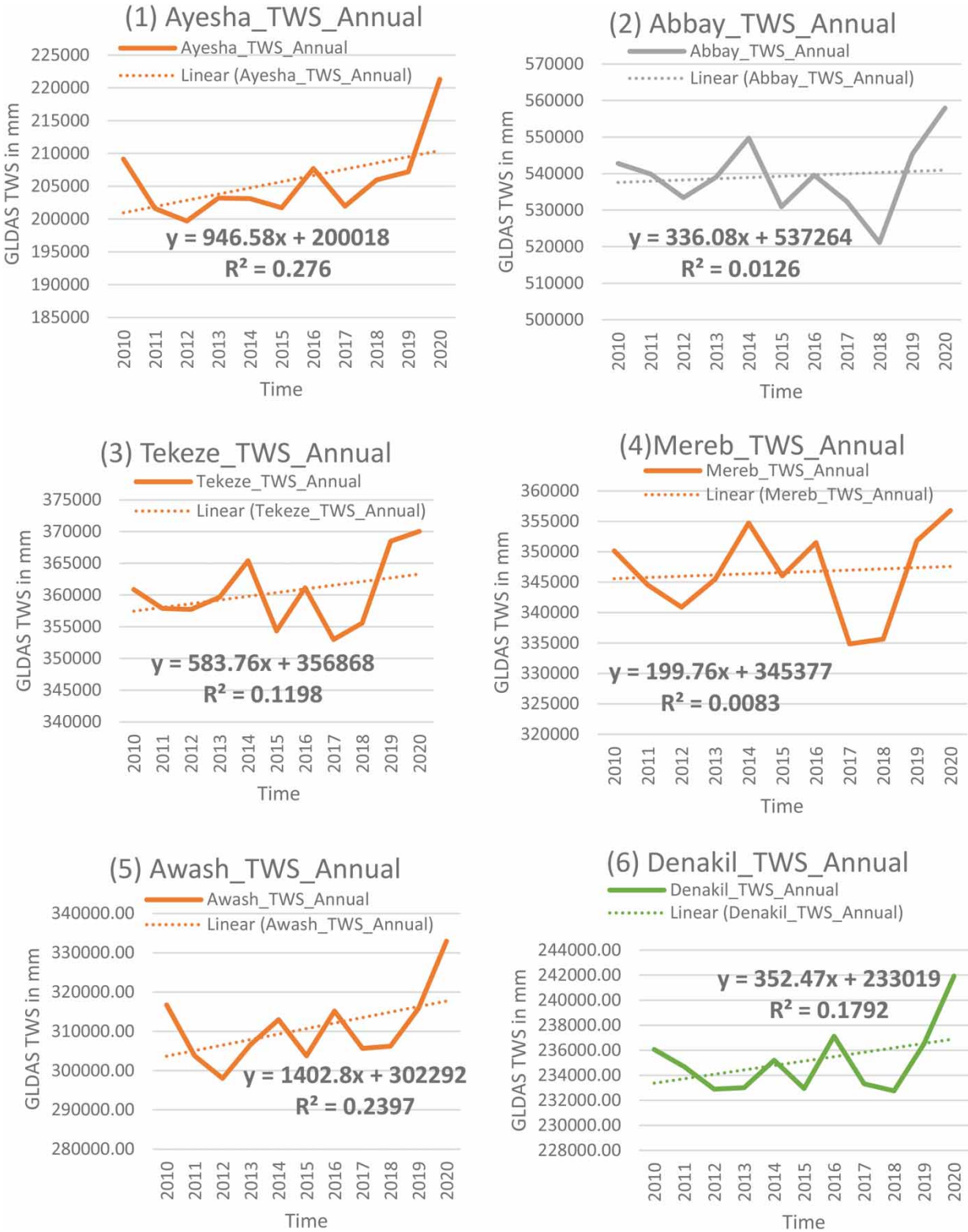

Figure 7 | Temporal variation of mean annual TWS from GLDAS for the major river basins of Ethiopia from 2010 to 2020. (1) Temporal variation of TWS for Ayesha, (2) temporal variation of TWS for Abbay, (3) temporal variation of TWS for Tekeze, (4) temporal variation of TWS for Mereb Gash, (5) temporal variation of TWS for Awash, (6) temporal variation of TWS for Denakil, (7) temporal variation of TWS for Ogaden, (8) temporal variation of TWS for Wabishebele, (9) temporal variation of TWS for Genale Dawa, (10) temporal variation of TWS for Rift Valley, (11) temporal variation of LWE for Omo-Gibe, and (12) temporal variation of TWS for Baro-Akobo. (*continued.*).

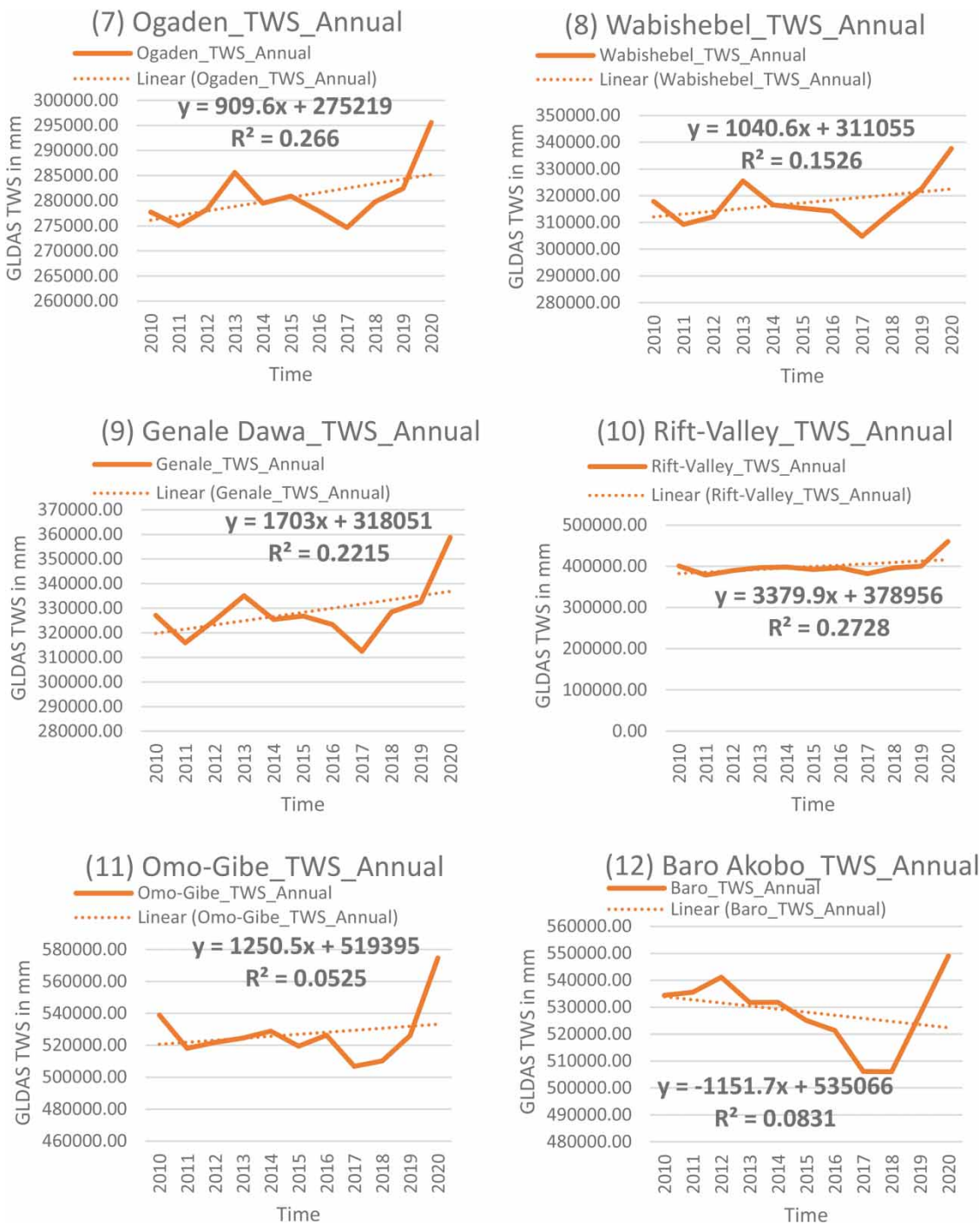

Figure 7 | Continued.

Tekeze, Mereb, Awash, Denakil, Rift Valley, Omo-Gibe, and Baro-Akobo; during Summer in Genale Dawa and Wabishebele, whereas minimum terrestrial water storage were observed in winter in Ayesha, Denakil, Genale Dawa, Wabishebele, and Ogaden); in spring and winter in Awash; and in spring in Abbay, Tekeze, Mereb, Rift-Valley, Omo-Gibe, and Baro-Akobo. The yearly trend of terrestrial water storage for each river basin from GLDAS dataset was evaluated using R-studio, and the result indicates a significant increasing trend during the entire study period for Ayesha (0.097, 1.85, 1.6×10^{-04}), Abbay (0.74, 0.33, 1.1×10^{-04}), Tekeze (0.09, 1.1, 1.85×10^{-04}), Mereb Gash (0.79, 0.27, 1.51×10^{-04}), Denakil (0.19,1.4,

3.63×10^{-04}), Awash (0.12,1.68, 1.01×10^{-04} and 0.10, 1.62×10^{-04}), Wabishebele (0.235, 1.27, 1.15×10^{-04}), Genale Dawa (0.144, 1.6, 8.12×10^{-05}), Omo-Gibe (0.49, 0.7, 5.9×10^{-05}), whereas a significant decreasing trend during the entire study period for Baro-Akobo (0.39, −0.9, 7.99×10^{-05}), Pr(>|*t*|)-value, *t*-value, and standard error, respectively, at 0.05 significance level.

3.2.2. Spatial distribution of terrestrial water storage from GLDAS

Figure 8 presents the average spatial distribution of terrestrial water storage from 2010 to 2020 for the major river basins of Ethiopia. Based on the result, the range of spatial distribution of terrestrial water storage for Abbay River Basin (Figure 8(1)) was from 628.16 to 2,311.5 mm with high storage in the southwestern part of the river basin, 450.82 to 1,812.63 mm for Tekeze (Figure 8(2)) with few high water storage in the northern parts and medium storage in central, southern, and western parts of the river basin, 817.424 to 1,087.07 mm for Mereb Gash (Figure 8(3)) with high storage in the eastern and low storage in the western part of the river basin, 378.8 to 1,451.28 mm for Denakil (Figure 8(4)) with high storage in the western part of the river basin, 505.89 to 1,845.28 mm with high storage in the south western part and low storage in the north eastern part of the river basin (Figure 8(5)), 544.29 to 725.37 mm with high storage in the north eastern part and the rest was with low storage (Figure 8(6)), 1,188.17 to 1,958.21 mm for Baro-Akobo with high storage in the north eastern part and declining towards the eastern direction (Figure 8(7)), 566.2 to 2,130.85 mm for Omo-Gibe with declining from northern towards to the southern part of the river basin (Figure 8(8)), 572.87 to 1,741.64 mm for Rift Valley with declining in storage from the north eastern to south western part (Figure 8(9)), 535.05 to 1,893.61 mm for Genale Dawa with low storage in south eastern, high storage in northern, and medium in south western parts of the river basin (Figure 8(10)), 523.78 to 1,867.04 mm for Wabishebele River Basin (Figure 8(11)) with increasing in storage from the south to north west part of the river basin, and 514.755 to 1,683.57 mm for Ogaden River Basin (Figure 8(12)) with high storage in the south eastern part and the rest experiencing low terrestrial water storage. The change in spatial distribution of water storage was observed for each river basin in the study period, and the variation of the water storage was observed due to overutilization of water for irrigation and domestic water supply, and different studies confirm this with other studies (Luo *et al*. 2016; Nie *et al.* 2016; Raghavendra & Cholke 2017).

3.2.3. Estimation of evapotranspiration from water balance equation

Estimation of evapotranspiration for a large river basin requires complex modeling and data analysis. There are various methods and models to estimate evapotranspiration, including the Penman–Monteith method, the Hargreaves method, and the Priestley Taylor method. These methods generally require data on weather variables such as temperature, humidity, wind speed, solar radiation, atmospheric pressure, as well as data on vegetation cover, soil moisture, and other factors. But, for this study, evapotranspiration for each river basin was evaluated by using a water balance, Equation (3), with an estimated GRACE dataset, and the results are presented in Figure 9. The result experiences rising and falling of evapotranspiration for each river basin. The result reveals that evapotranspiration in all river basins changes by simultaneous rising and falling. The yearly trend of the evapotranspiration for each river basin shows a decreasing trend for all river basins except Baro-Akobo.

3.2.4. Characteristics of precipitation, temperature, evapotranspiration, and LWE for each river basin

To understand the effect of climatic variables (temperature, precipitation, and evapotranspiration) on terrestrial water storage, cross-correlation between each parameter for individual river basins was evaluated, and the result of the six most relevant cross-correlations is discussed in this article. Figure 10 shows the cross-correlation of climatic values for the Abbay River Basin.

The result of cross-correlation shown in Figure 10 demonstrates that the cross-correlation for Abbay river (0.96, 0.83, 0.8, −0.76, 0.76, −0.75) between (Pr + TWS), (TWS + EVT), (Pr + EVT), (Pr + aet), and (Pr + tmx), respectively; Ayesha river (1, 0.998, 0.997, −0.87, 0.44, 0.441) between (Pr + aet), (Pr + TWS), (aet + TWS), (LWE + EVT), (TWE + tmx), and (Pr + tmx), respectively; Mereb Gash river (0.92, 0.92, 0.81, 0.80, 0.79, −0.69) between (Pr + aet), (Pr + EVT), (aet + EVT), (Pr + TWS), (TWS + EVT), and (LWE + tmx), respectively; Tekeze river (0.89, 0.88, 0.87, 0.86, −0.72, −0.7) between (Pr + TWS), (Pr + aet), (Pr + EVT), (TWS + EVT), and (LWE + tmx), respectively. Denakil river (0.98, 0.89, 0.78, −0.68, 0.62, 0.56) between (Pr + aet), (Pr + TWS), (aet + TWS), (LWE + EVT), (TWS + EVT), and (Pr + EVT), respectively. The positive cross-correlation shows the variable was a direct relationship, but the negative cross-correlation indicates an indirect relationship between the variables.

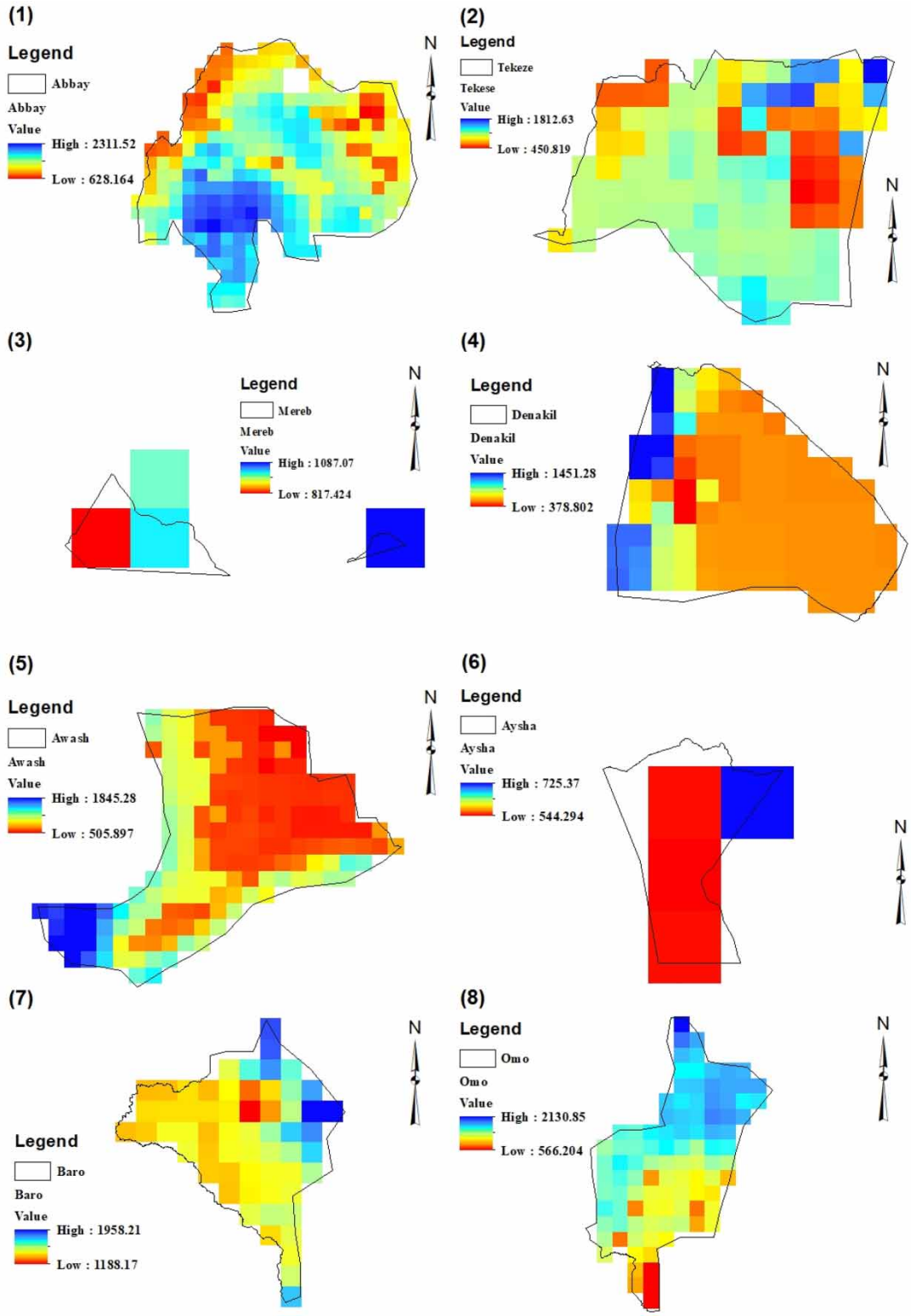

Figure 8 | Spatial variation of average TWS from GLDAS for the 12 river basins of Ethiopia from 2010 to 2020. (1) Spatial distribution of TWS for Abbay, (2) spatial distribution of TWS for Tekeze, (3) spatial distribution of TWS for Mereb Gash, (4) spatial distribution of TWS for Denakil, (5) spatial distribution of TWS for Awash, (6) spatial distribution of TWS for Aysha, (7) spatial distribution of TWS for Baro-Akobo, (8) spatial distribution of TWS for Omo-Gibe, (9) spatial distribution of TWS for Rift Valley, (10) spatial distribution of TWS for Genale Dawa, (11) spatial distribution of TWS for Wabishebel, and (12) spatial distribution of TWS for Ogaden. (*continued.*).

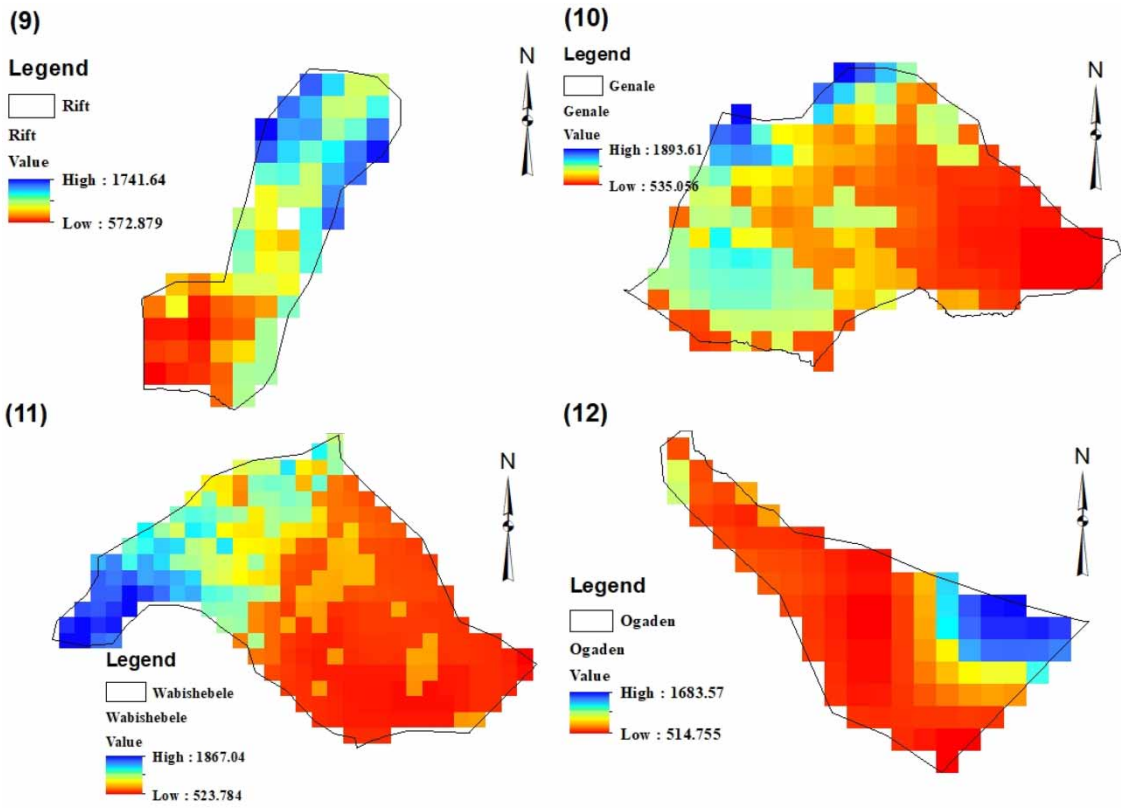

Figure 8 | Continued.

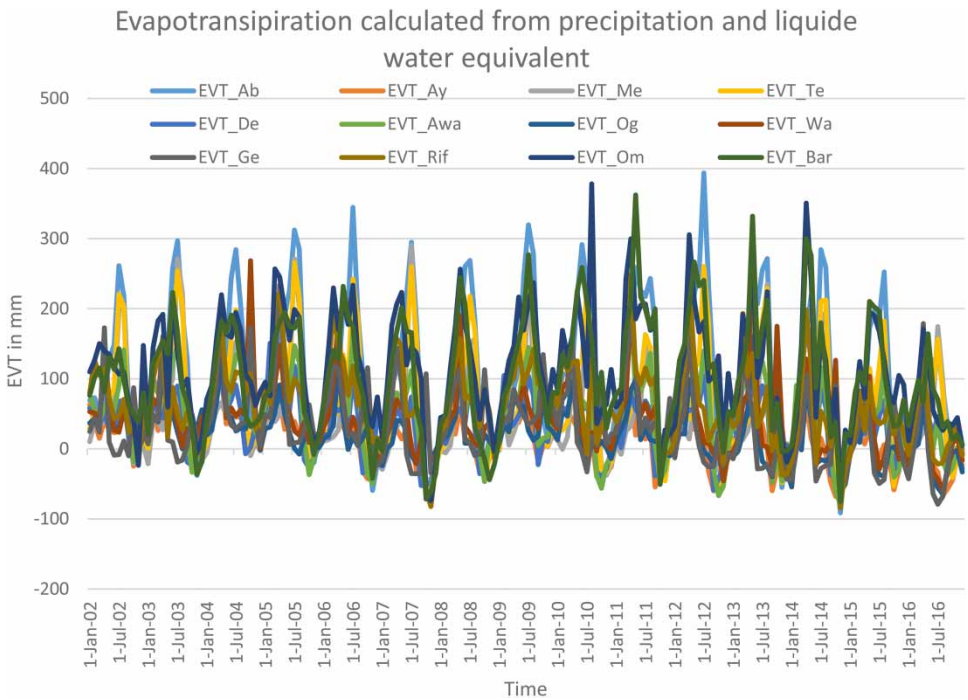

Figure 9 | Evapotranspiration for the major river basins of Ethiopia.

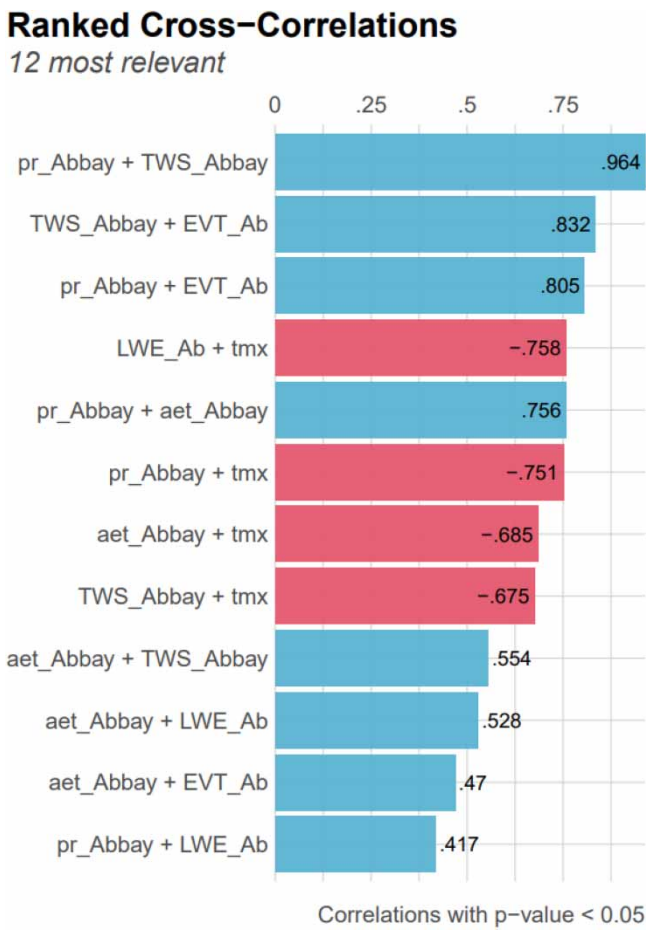

Figure 10 | Cross-correlation for the climatic variable with TWS and LWE. Pr is precipitation, aet is actual evapotranspiration, EVT is evapotranspiration obtained from GRACE dataset and precipitation, tmx is the maximum temperature, LWE is liquid water equivalent from GRACE dataset, and TWS is terrestrial water storage estimated from precipitation and actual evapotranspiration.

3.2.5. Factors affecting the decrease in LWE and TWS for the major river basins

Based on the result described earlier, the relationship between precipitation, evapotranspiration, actual evapotranspiration, and temperature with LWE and TWS is presented in Figure 11. The general increase in temperature and evapotranspiration and the decrease in precipitation agreed with negative liquid water equivalent and terrestrial water storage for all river basins. In terms of the variability rate, we observed evapotranspiration was nearly twice as high as precipitation, which indicates that evapotranspiration is more sensitive to LWE and TWS dynamics. In addition, an increase in temperature shows a negative correlation between LWE and TWS. According to Zhang *et al.* (2015), an increase in surface temperature enhanced the evapotranspiration, so the drought was strengthened during the period and our result agree with this finding (Kalma *et al.* 2008; Herrmann *et al.* 2015; Huang *et al.* 2015; Chupin & Yoshe 2022; Lemma *et al.* 2022).

3.2.6. Advantages and disadvantages of GRACE dataset in terrestrial water storage

Hydrological prediction depends on knowledge of initial hydrological conditions. Traditionally, the analysis and prediction of hydrological extremes have involved statistical assessments of long-term climatic and hydrological datasets to evaluate flood thresholds, severity, recurrence intervals, and drought events. Efforts to improve hydrological prediction and reduce uncertainty can now leverage a wealth of new tools for measurement and estimation of land surface states, namely, satellite remote sensing products and advanced numerical models (Famiglietti *et al.* 2015; Li *et al.* 2019). The GRACE satellite mission has been an important step forward in observing terrestrial water storage with global coverage. GRACE provides monthly data on change in the Earth's gravity field, which we assume is correlated with the movement of water through the Earth's system at specific temporal and spatial scales. GRACE has been providing monthly gravity field solutions since April 2002 and has

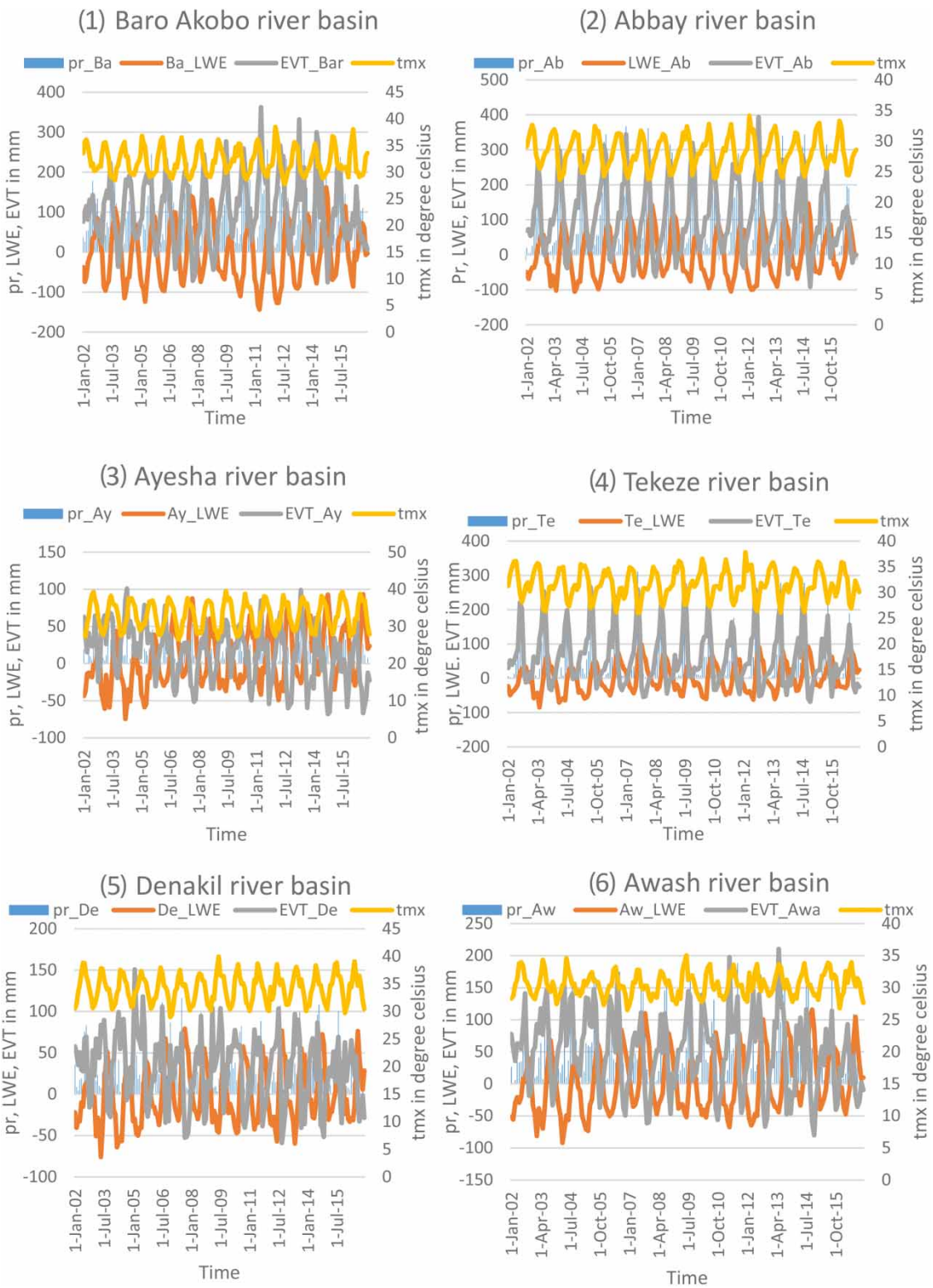

Figure 11 | Characteristics of precipitation, liquid water equivalent, evapotranspiration, and maximum temperature: (1) Baro-Akobo River Basin, (2) Abbay River Basin, (3) Ayesha River Basin, (4) Tekeze River Basin, (5) Denakil River Basin, (6) Awash River Basin, (7) Ogaden River Basin, (8) Wabishebele River Basin, (9) Genal Dawa River Basin, (10) Rift Valley River Basin, (11). Omo-Gibe River Basin, and (12) Baro-Akobo River Basin. (*continued.*).

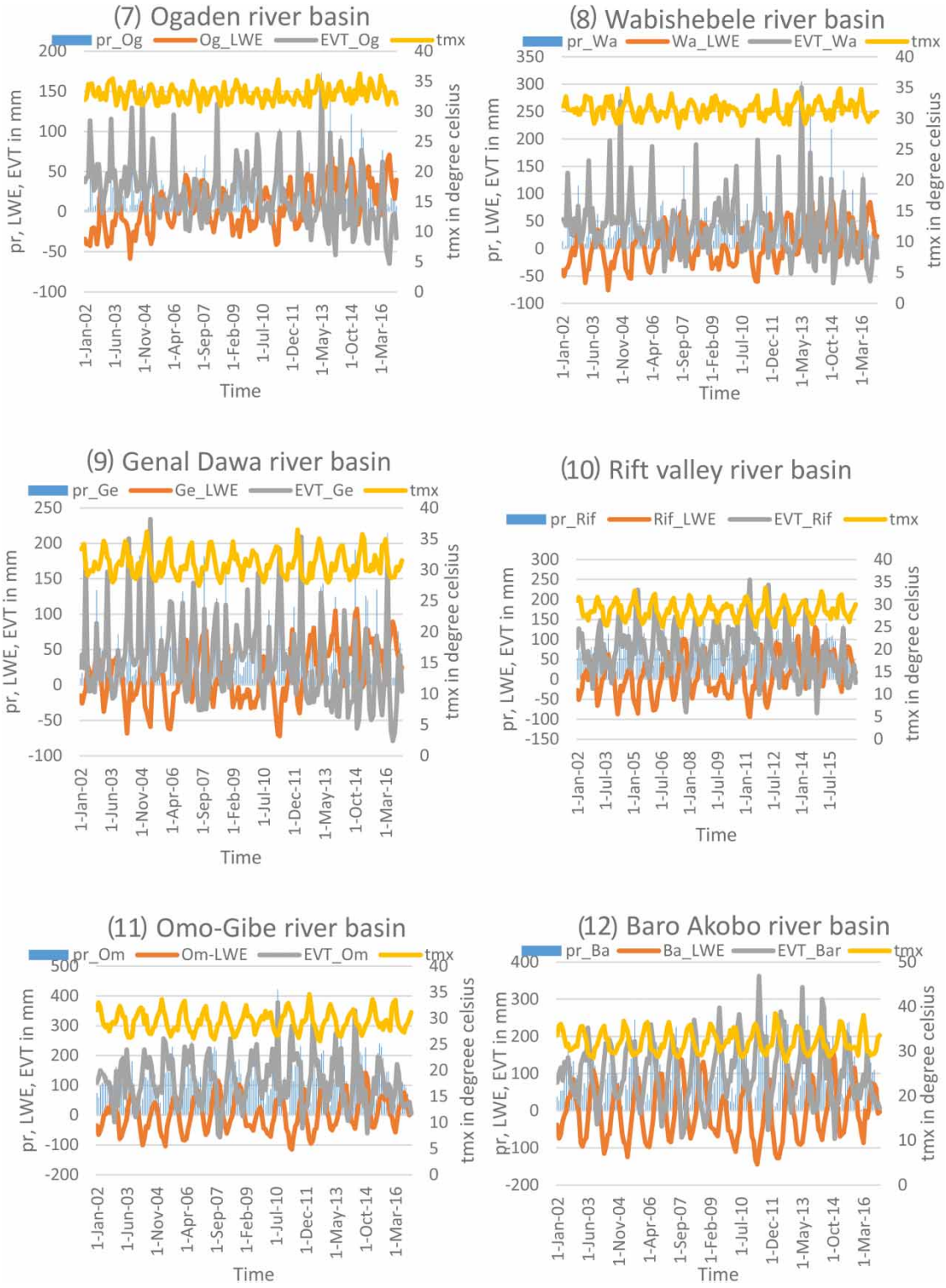

Figure 11 | Continued.

proved an effective tool to observe changes in the mass of ice, snow, groundwater storage, surface water storage, and hydrologic drought characterization, which is confirmed by different research studies (Kim *et al.* 2009; Houborg *et al.* 2012; Li *et al.* 2012; Thomas *et al.* 2014; Richey *et al.* 2015). GRACE has also contributed to flood estimation, which is consistent with

different findings (Reager & Famiglietti 2009; Reager *et al.* 2014). GRACE terrestrial water storage anomaly data can contribute to an improved understanding of soil moisture and groundwater contributions to future runoff generation, but the utility of GRACE data for operational analysis or actionable prediction is challenging. Three prevailing limitations are as follows: (1) coarse spatial resolution that shows one arc-degree for the level-three data product (Landerer & Swenson 2012; Famiglietti *et al.* 2015); (2) the aggregated observation of multiple water storage components as a single integrated value for each grid cell; and (3) latency in data product processing and release (Reager & Famiglietti 2009; Gebere *et al.* 2015). These obstacles make many applications difficult, as water resource management trends occur at watershed scales and on daily to weekly timescales. Assimilation of GRACE observations enable spatial, vertical, and temporal disaggregation of terrestrial water storage components, including groundwater, surface water, root zone soil moisture, and snow, while preserving the internal consistency of the modeled storages and fluxes and taking into account uncertainties due to model and observational errors. Model uncertainty is caused by errors in surface meteorological forcing, model parameters, and model structural errors. Some of the uncertainty is related to unmodeled processes, most notably human impacts such as pumping groundwater, irrigation water supply, domestic water use, and water management practices, which are not considered by GRACE satellite. Therefore, it is common to rescale the observations prior to data assimilation to address model and observation biases. Such rescaling may discard important signals in the observation and make it difficult to isolate errors caused by unmodeled processes including true observational features for data assimilation, which is also confirmed by different findings (Reichle & Koster 2004; Zaitchik *et al.* 2008; Ozdogan *et al.* 2010; Kumar *et al.* 2015; Zhou *et al.* 2016). The water crisis is one of the main global risks that has different impacts on society. This study uses available data and tools to track water storage change in the area, where there is a lack of observations and limited hydro climatological studies. The GLDAS and GRACE datasets were globally used in water resources and climate studies, particularly in areas where data are temporally and spatially limited. Therefore, the application of GRACE data and GLDAS provides a new research approach to explore change in water storage throughout the world for areas with scare datasets and also for Ethiopia in particular. Different studies throughout the world evaluated water storage variations for larger watersheds (Zaitchik *et al.* 2008; Yoshe 2023) and even groundwater storage (Rodell *et al.* 2007). The result of the study adds high value for the study area to monitor drought events, hydrological extremes, and chemotic changes, and it is also very essential for water resource management and optimization. As agriculture was the backbone of Ethiopian economic development, this finding creates valuable information for water resource planners and decision-makers.

3.2.7. Terrestrial water storage anomalies decomposition using ICA

We performed ICA on terrestrial water storage anomalies for each river basin and obtained two leading modes (the trend and annual modes). Since the ranking of the components obtained by ICA corresponds to a random ordering instead of a reduction in variance, we estimated the average ratio of the contribution of each IC to the observed unfiltered time series in order to reorder ICA components in the ascending order for each river basin, and the spatial portion of each ICA result is normalized by its maximum value. For each river basin, the annual mode, which explains more than 80% of the total variance of the filtered terrestrial water storage anomalies time series, is followed by the trend mode, which explains less than or equal to 20% of the total variance for each river basin. The spatial weight of the IC shows a positive and negative contribution to the corresponding time functions for each river basin based on spatial water variation in each river basin, climatic change, and anthropogenic activities. The negative and positive weights correspond to decreasing and increasing water storage in the study area, which may be affected by distributions of land use, land cover, population density, precipitation, soil type, and different human activities in each river basin.

3.2.8. Comparison of the ICA model with simulated climatic water storage anomalies and Humphrey water storage anomaly products

For each river basin, the annual mode and the trend mode show the seasonal fluctuation in water storage anomalies. Our results are generally consistent with the Humphrey result of terrestrial water storage anomalies Equation (5) (Humphrey *et al.* 2017), which are affected by climate variability, with an R^2 value for each river basin greater than 85%. This shows that the climatic water storage anomalies in the major river basins of Ethiopia can be explained by the annual mode and the trend mode, respectively, and that ICA may provide a new method to isolate the impact of climatic variability and human activities on water storage variation. For each river basin, the maximum seasonal water storage fluctuations and the average amplitude of climatic water storage anomalies from GRACE and the GLDAS model vary from each other

because the climatic water storage anomalies derived from GRACE, based on ICA, integrate all surface and subsurface water storages, whereas the GLDAS hydrological model contains soil moisture estimates from the surface to a certain depth, surface runoff, canopy water storage, and others, excluding the contribution of reservoir and groundwater storage. Each river basin has experienced a similar climate with little variation in drying and warming climates, and the impacts of climate change on terrestrial water storage anomalies have good consistency. During the dry season for each river basin, the climatic-derived water storage loss rates are very high, whereas in each river basin, water storage increases were observed during the wet season. This comes in response to precipitation fluctuation, which indicates that precipitation was the dominant driving force for the terrestrial water storage depletion in each river basin. Water storage anomalies with and without human interventions are used for each river basin to further isolate the effects of human intervention on terrestrial water storage anomalies. The result of human-driven water storage anomalies is consistent with the result of the statistical data yearbook. The primary causes of variation in terrestrial water storage are the effects of human interventions, which are mainly based on irrigation data and other activities. Scanlon *et al.* (2018) also suggest that global models underestimate large decadal declining and rising water storage trends relative to GRACE satellite data, and our result was consistent with these findings.

Each river basin has experienced significant increases in mining, irrigation, grazing, urbanization, hydropower construction, industrial activities, and other human activities. Overgrazing caused grassland degradation and resulted in a decrease in soil moisture retention capacity and groundwater depletion in each river basin, which is also confirmed by similar findings (Tao *et al.* 2015). The increase in irrigation expansions is highly increasing in each river basin and has caused extensive groundwater withdrawals, which is consistent with similar studies (Tao *et al.* 2015; Zhong *et al.* 2019). Coal mining is the most important product for economic development, and these activities were increasing in each river basin, which is an extremely water-intensive industry; each ton of coal mined more than 2.54 m^3 of water, which may cutoff rivers and destroy underground aquifers, as confirmed by similar studies (Tao *et al.* 2015; Liu *et al.* 2021). Compared to the rapid expansion of farmland due to increasing population growth in each river basin of Ethiopia, the agricultural area was increasing in each river basin, which added stress on water storage. The difference in population density in each river basin leads to a huge difference in the human intervention on water storage variation. In wet seasons, the impact of human activities on land water storage may be offset by climate changes; in dry seasons, intensive human activities may lead to a further decrease in terrestrial water storage in each river basin of Ethiopia, which will exacerbate drought and cause several ecological problems, including a sharp decrease in surface runoff, shrinking lakes and reservoirs, and intensifying desertification. It is crucial to take effective measures to protect these precious land water resources and prevent their further deterioration in each river basin in Ethiopia. This study provides a potential method to quantify the climate- and human-driven water storage variations in the major river basins of Ethiopia. It is of great significance for helping people better understand the evaluation of terrestrial water storage anomalies under the combined influence of climatic change and anthropogenic activities and providing information for better protection and utilization of water resources at river basin level. It will also help to facilitate basin (regional) sustainable water resource management and protection.

4. CONCLUSION

In this study, we used the GRACE dataset to evaluate LWE for major river basins of Ethiopia from 2002 to 2016. Combining with the GLDAS hydrological model, we evaluated the spatiotemporal variation of terrestrial water storage. The impact of climatic parameters on the terrestrial water storage was evaluated, and the following conclusions were drawn.

From the perspective of interannual variation, the liquid water equivalent shows a continuous increase and decrease, which indicates a distinct seasonal cycle. The liquid water equivalent gets its peak in the rainy season for each river basin, whereas it gets its lowest value during the dry season. The maximum and minimum LWE for each river basin, the monthly variation, and the spatial distribution of LWE for each river basin were evaluated for this study. The spatial distribution of LWE for Abbay ranges from −2.07 to 0.68 cm/month, Tekeze (−0.44 to 1.04 cm/month), Mereb Gash (−0.44 to 0.47 cm/month), Denakil (−0.82 to 1.04 cm/month), Awash (−0.41 to 1.85 cm/month), Ayesha (1.46 cm/month), Baro-Akobo (−2.1 to 2.43 cm/month), Omo-Gibe (−1.42 to 4.41 cm/month), Rift Valley (0.82 to 4.89 cm/month), Genale Dawa (2.78 to 5.6 cm/month), Wabishebele (0.69 to 3.57 cm/month), and Ogaden (1.45 to 2.11 cm/month). In addition, the overall trend in the study area was evaluated for each river basin. The annual water storage for each river basin was fluctuating in the study area. We understand that liquid water equivalents derived from GRACE show both the potential to reveal changes in terrestrial water storage and the ability to support hydrological modeling. In addition, from the GLDAS land state surface variables,

water storage change was estimated for all river basins. For estimation of water storage change from the GLDAS dataset, soil moisture (surface soil moisture, profile soil moisture, and root zone soil moisture), canopy water storage, and surface water storage are the variables used. The time series of the estimated water storage for the mean monthly water storage for each river basin evaluated shows continuous rising and falling, showing the seasonal pattern of the study area. The evaluated liquid water storage from GRACE datasets and GLDAS was compared for each river basin. There is a match for the seasonal peak and low of water storage for each river basin. However, interannual variation shows a significant difference in each river basin for some months of study periods. The cross-correlation coefficient between water storage from GRACE and GLDAS for each river basin was evaluated.

Under the background of intensive climate warming and human activities, quantifying water storage dynamic process is a key issue for ecologically fragile areas such as the major river basins of Ethiopia, this work implicated that it is possible to access the impact of climate change and human activities on terrestrial water storage anomaly changes through the ICA method and multi-sources datasets. It can help manage and protect water resources and provide possible solutions for sustainable ecological and socioeconomic development.

The increase in evapotranspiration was also the dominant factor contributing to the decrease in LWE/TWS for each river basin, while the decrease in precipitation had a certain effect on LWE/TWS as well. We observed that an increase in temperature causes a decrease in terrestrial water storage for all river basins. We concluded that climate change and anthropogenic activity influence terrestrial water storage, mainly precipitation, temperature, and evapotranspiration. Finally, we prove that GRACE satellite provides users with valued data even in areas where available data are limited. In addition, the GLDAS dataset also provides the necessary dataset for estimating the water budget of an area. The quantified result demonstrates that understanding the spatiotemporal distribution is important to avoid water crises in future, and conserve natural water resources by monitoring the water storage. Policymakers and researchers also benefited from this finding as baseline information for the study area.

FUNDING

This research did not receive any specific grant from funding agencies in the public, commercial or nonprofit sectors.

DATA AVAILABILITY STATEMENT

Data cannot be made publicly available; readers should contact the corresponding author for details.

CONFLICT OF INTEREST

The authors declare there is no conflict.

REFERENCES

Abboye, A. D. 2021 Review study on current bread wheat (*Triticum aestivum* L.) production status and Key challenges for potential efficiency of wheat markets in Ethiopia. *Journal of Ecology & Natural Resources* **5** (2). doi:10.23880/jenr-16000233.

Alemu, A. M., Seleshi, Y. & Meshesha, T. W. 2022 Modeling the spatial and temporal availability of water resources potential over Abbay river basin, Ethiopia. *Journal of Hydrology: Regional Studies* **44**, 101280.

Altaseb, A. & Singh, K. 2018 Economic growth determinants in Ethiopia: A literature survey. *International Journal of Research and Analytical Reviews* **5** (4), 326–336.

Awulachew, S. B., Yilma, A. D., Loulseged, M., Loiskandl, W., Ayana, M. & Alamirew, T. 2007 *Water Resources and Irrigation Development in Ethiopia*. International Water Management Institute, Colombo, Sri Lanka, p. 78. (Working Paper 123)

Bartle, A. 2002 Hydropower potential and development activities. *Energy Policy* **30** (14), 1231–1239.

Bayissa, Y., Moges, S., Xuan, Y., Van Andel, S., Maskey, S., Solomatine, D., Griensven, A. & Tadesse, T. 2015 Spatiotemporal assessment of meteorological drought under the influence of varying record length: The case of Upper Blue Nile Basin, Ethiopia. *Hydrological Sciences Journal* **60** (11), 1927–1942. https://doi.org/10.1080/02626667.2015.1032291.

Bayissa, Y., Tadesse, T., Demisse, G. & Shiferaw, A. 2017 Evaluation of satellite-based rainfall estimates and application to monitor meteorological drought for the Upper Blue Nile Basin. *Ethiopian Remote Sensing* **9** (7), 669. https://doi.org/10.3390/rs9070669.

Belkhiri, L., Tiri, A. & Mouni, L. 2018 Chapter 2. Assessment of heavy metals contamination in groundwater: A case study of the South of Setif Area, East Algeria. Books. In: *Achievements and Challenges of Integrated River Basin Management*, pp. 17–31. Available from: http://dx.doi.org/10.5772/intechopen.75734.

Bingham, E. & Hyvärinen, A. 2000 A fast fixed-point algorithm for independent component analysis. *International Journal of Neural Systems* **10**, 1–8.

Chao, N., Luo, Z., Wang, Z. & Jin, T. 2018 Retrieving groundwater depletion and drought in the Tigris-Euphrates Basin between 2003 and 2015. *Groundwater* **56** (5), 770–782. https://doi.org/10.1111/gwat.12611.

Chen, J. L., Wilson, C. R., Tapley, B. D., Scanlon, B. & Guentner, A. 2016 Long-term groundwater storage change in Victoria, Australia from satellite gravity and in situ observations. *Global and Planetary Change* **139**, 56–65.

Chen, L., He, Q., Liu, K., Li, J. & Jing, C. 2019 Downscaling of GRACE-derived groundwater storage based on the random forest model. *Remote Sensing* **11**, 2979.

Chupin, V. R. & Yoshe, A. K. 2022 Seasonal water balance of the Abay River Basin assessed using satellite databases and a specialized hydrological model. *Izvestiya Vuzov. Investitsii. Stroitel'stvo. Nedvizhimost' = Proceedings of Universities. Investment. Construction. Real Estate.* **12** (4), 606–616. (In Russ.). https://doi.org/10.21285/2227-2917-2022-4-606-616.

Dai, Y., Zeng, X., Dickinson, R. E., Baker, I., Bonan, G. B., Bosilovich, M. G. & Oleson, K. W. 2013 The common land model. *Bulletin of the American Meteorological Society* **84**, 1013–1024.

De Beurs, K. M., Henebry, G. M., Owsley, B. C. & Sokolik, I. 2015 Using multiple remote sensing perspectives to identify and attribute land surface dynamics in Central Asia 2001–2013. *Remote Sensing of Environment* **170**, 48–61.

Degefu, D. M., He, W. & Zhao, J. H. 2015 Hydropower for sustainable water and energy development in Ethiopia. *Sustainable Water Resource Management*. doi:10.1007/s40899-015-0029-0.

Edossa, D., Babel, M. & Das Gupta, A. 2010 Drought analysis in the Awash River Basin, Ethiopia. *Water Resources Management* **24** (7), 1441–1460. https://doi.org/10.1007/s11269-009-9508-0.

Ek, M. B., Mitchell, K. E., Lin, Y., Rogers, E., Grunmann, P., Koren, V. & Tarpley, J. D. 2003 Implementation of Noah land surface model advances in the National Centers for Environmental Prediction operational mesoscale Eta model. *Journal of Geophysical Research: Atmospheres* **2003**, 108.

Famiglietti, J. S., Cazenave, A., Eicker, A., Reager, J. T., Rodell, M. & Velicogna, I. 2015 Satellites provide the 'Big picture' for global hydrology. *Science* **349**, 684–685.

Fasullo, J. T., Lawrence, D. M. & Swenson, S. C. 2016 Are GRACE-era terrestrial water trends driven by anthropogenic climate change? *Advances in Meteorology* **2016**, 4830603.

Felfelani, F., Wada, Y., Longuevergne, L. & Pokhrel, Y. N. 2017 Natural and human-induced terrestrial water storage change: A global analysis using hydrological models and GRACE. *Journal of Hydrology* **553**, 105–118.

Feng, W., Wang, C. Q., Mu, D. P., Zhong, M., Zhong, Y. L. & Xu, H. Z. 2017 Groundwater storage variations in the North China Plain from GRACE with spatial constraints. *Chinese Journal of Geophysics* **60**, 1630–1642.

Frappart, F. & Ramillien, G. 2018 Monitoring groundwater storage changes using the gravity recovery and climate experiment (GRACE) satellite mission: A review. *Remote Sensing* **10**, 829.

Frappart, F., Ramillien, G. & Ronchail, J. 2013 Changes in terrestrial water storage versus rainfall and discharges in the Amazon basin. *International Journal of Climatology* **33**, 3029–3046.

Gebere, S., Alamirew, T., Merkel, B. & Melesse, A. 2015 Performance of high-resolution satellite rainfall products over data scarce parts of Eastern Ethiopia. *Remote Sensing* **7** (9), 11639–11663. https://doi.org/10.3390/rs70911639.

Gebrehiwot, T., van der Veen, A. & Maathuis, B. 2011 Spatial and temporal assessment of drought in the northern highlands of Ethiopia. *International Journal of Applied Earth Observation and Geoinformation* **13** (3), 309–321. https://doi.org/10.1016/j.jag.2010.12.002.

Geda, K., Douglas, M., Rita, B. L., Olyad, D., Aschalew, L., Daniel, S. H., Andreas, H. F. & Wolfram, G. 2020 Macroinvertebrate indices versus microbial fecal pollution characteristics for water quality monitoring reveals contrasting results for an Ethiopian river. *Ecological Indicators* **108**, 105733.

Gidey, E., Dikinya, O., Sebego, R., Segosebe, E. & Zenebe, A. 2018 Modelling the spatio-temporal meteorological drought characteristics using the standardized precipitation index (SPI) in Raya and its Environs Northern Ethiopia. *Earth Systems and Environment* https://doi.org/10.1007/s41748-018-0057-7.

Golmohammadi, G., Rudra, R., Prasher, S., Madani, A., Mohammadi, K., Goel, P. & Daggupatti, P. 2017 Water budget in a tile drained watershed under future climate change using SWATDRAIN model. *Journal of Climate* **5** (2), 39. www.mdpi.com/2225-1154/5/2/39

Gunkel, A., Shadeed, S., Hartmann, A., Wagener, T. & Lange, J. 2015 Model signatures and aridity indices enhance the accuracy of water balance estimation in a data-scarce Eastern Mediterranean catchment. *Journal of Hydrology and Regional Study* **4** (Part B), 487–501.

Gupta, A., Thakur, P. K., Nikam, B. R. & Chouksey, A. 2014 Water Balance Study of Narmada River Basinan Integrated Approach Using Remote Sensing and GIS Tools and Techniques. In: *3rd National Conference on Trends and Recent Advances in Civil Engineering at: Noida, India Volume: Proceedings of TRACE-2014*.

Herrmann, F., Keller, L., Kunkel, R., Vereechen, H. & Wendland, F. 2015 Determination of spatially differentiated water balance components including groundwater recharge on the Federal State level – A case study using them GROWA model in North Rhine-Westphalia (Germany). *Journal of Hydrology and Regional Study* **4** (Part-B), 294–312.

Houborg, R., Rodell, M., Li, B., Reichle, R. & Zaitchik, B. F. 2012 Drought indicators based on model-assimilated Gravity Recovery and Climate Experiment (GRACE) terrestrial water storage observations. *Water Resources Research* **48**, W07525. doi: https://doi.org/10.1029/2011WR011291.

Hsu, Y.-J., Fu, Y. N., Bürgmann, R., Hsu, S.-Y., Lin, C.-C., Tang, C.-H. & Wu, Y.-M. 2020 Assessing seasonal and interannual water storage variations in Taiwan using geodetic and hydrological data. *Earth and Planetary Science Letters* **550**, 116532.

Hu, W., Liu, H., Bao, A. & El-Tantawi, A. M. 2018 Influences of environmental changes on water storage variations in Central Asia. *Journal of Geographical Sciences* **28**, 985–1000.

Huang, Y., Salama, M. S., Krol, M. S., Su, Z., Hoekstra, A. Y., Zeng, Y. & Zhou, Y. 2015 Estimation of human-induced changes in terrestrial water storage through integration of GRACE satellite detection and hydrological modeling: A case study of the Yangtze River basin. *Water Resources Research* **51**, 8494–8516.

Humphrey, V. & Gudmundsson, L. 2019 GRACE-REC: A reconstruction of climate-driven water storage changes over the last century. *Earth System Science Data* **11**, 1153–1170.

Humphrey, V., Gudmundsson, L. & Seneviratne, S. I. 2017 A global reconstruction of climate-driven subdecadal water storage variability. *Geophysical Research Letters* **44**, 2300–2309.

Hyvarinen, A. 1999 Fast and robust fixed-point algorithms for independent component analysis. *IEEE Transactions on Neural Networks* **10**, 626–634.

Hyvarinen, A. & Oja, E. 2000 Independent component analysis: Algorithms and applications. *Neural Networks* **13**, 411–430.

Jasrotia, S., Majhi, A. & Singh, S. 2009 Water balance approach for rainwater harvesting using remote sensing and GIS techniques, Jammu Himalaya, India. *Journal of Water Resource Management Springer* **23**, 3035–3055.

Jenifa, L. C., Saravanan, S. & Palanichamy, K. 2010 A semi-distributed water balance model for Amravati River Basin using remote sensing and GIS. *International Journal of Geomatics and Geosciences* **1** (2), 252–263.

Jian, S. Q., Zhao, C. Y., Fang, S. M. & Yu, K. 2015 Effects of different vegetation restoration on soil water storage and water balance in the Chinese Loess Plateau. *Journal of Agriculture for Meteorology* **206**, 85–96.

Kalma, J., McVicar, T. & McCabe, M. 2008 Estimating land surface evaporation: A review of methods using remotely sensed surface temperature data. *Surveys in Geophysics* **29**, 421–469.

Kanga, S. 2017 Forest cover and land use mapping using remote sensing and GIS Technology. *Suresh Gyan Vihar University Journal of Climate Change and Water* **1** (2), 13–17.

Katpatal, Y. B., Rishma, C. & Singh, C. K. 2018 Sensitivity of the gravity recovery and climate experiment (GRACE) to the complexity of aquifer systems for monitoring of groundwater. *Hydrogeology Journal* **26**, 933–943.

Khaki, M., Forootan, E., Kuhn, M., Awange, J., Dijk, V., Schumacher, A. I. J. M. & Sharifi, M. A. M. 2018 Determining water storage depletion within Iran by assimilating GRACE data into the W3RA hydrological model. *Advances in Water Resources* **114**, 1–18.

Khandu, E., Forootan, M., Schumacher, J., Awange, L. & Müller Schmied, H. 2016 Exploring the influence of precipitation extremes and human water use on total water storage (TWS) changes in the Ganges-Brahmaputra-Meghna River Basin. *Water Resources Research* **52**, 2240–2258.

Kim, H., Yeh, P. J. F., Oki, T. & Kanae, S. 2009 Role of rivers in the seasonal variations of terrestrial water storage over global basins. *Geophysical Research Letters* **36**, L17402. doi:https://doi.org/10.1029/2009GL039006.

Klees, R., Zapreeva, E. A., Winsemius, H. C. & Savenije, H. H. G. 2007 The bias in GRACE estimates of continental water storage variations. *Hydrology and Earth System Sciences* **11**, 1227–1241.

Koster, R. D. & Suarez, M. J. 2022 Energy and water balance calculations in the Mosaic LSM. NOAA, Goddard Space Flight Center, Laboratory for Atmospheres, Data Assimilation Office: Laboratory for Hydrospheric Processes. Available from: https://gmao.gsfc.nasa.gov/pubs/docs/Koster130.pdf (accessed 5 October 2022).

Kumar, S., Peters-Lidard, C., Santanello, J., Reichle, R., Draper, C., Koster, R., Nearing, G. & Jasinski, M. 2015 Evaluating the utility of satellite soil moisture retrievals over irrigated areas and the ability of land data assimilation methods to correct for unmodeled processes. *Hydrology and Earth System Sciences* **19** (11), 4463.

Kumar, A., Kanga, S. & Sudhanshu 2018 Water balance assessment using geospatial techniques: A review. *i-manager's Journal on Future Engineering and Technology* **14** (1), 55.

Landerer, F. W. & Swenson, S. C. 2012 Accuracy of scaled GRACE terrestrial water storage estimates. *Water Resources Research* **48**, W04531.

Lemma, E., Upadhyaya, S. & Ramsankaran, R. 2022 Meteorological drought monitoring across the main river basins of Ethiopia using satellite rainfall product. *Environmental Systems Research* 2–15. https://doi.org/10.1186/s40068-022-00251-x.

Li, B., Rodell, M., Zaitchik, B., Reichle, R., Koster, R. & van Dam, T. 2012 Assimilation of GRACE terrestrial water storage into a land surface model: Evaluation and potential value for drought monitoring in western and central Europe. *Journal of Hydrology* **446–447**, 103–115. https://doi.org/10.1016/j.jhydrol.2012.04.035.

Li, Q., Luo, Z. C., Zhong, B. & Wang, H. H. 2013 Terrestrial water storage changes of the 2010 southwest China drought detected by GRACE temporal gravity field. *Chinese Journal of Geophysics* **56**, 1843–1849.

Li, W., Wang, W., Zhang, C. Y., Yang, Q., Feng, W. & Liu, Y. 2018 Monitoring groundwater storage variations in the Guanzhong area using GRACE satellite gravity data. *Chinese Journal of Geophysics* **6**, 2237–2245.

Li, B., Rodell, M., Kumar, S., Beaudoing, H. K., Getirana, A., Zaitchik, B. F., de Goncalves, L. G., Cossetin, C., Bhanja, S., Mukherjee, A., Tian, S., Natthachet Tangdamrongsub, D. L., Nanteza, J., Lee, J., Policelli, F., Goni, I. B., Daira, D., Bila, M., de Lannoy, G., Mocko, D., Steele-Dunne, S. C., Save, H. & Bettadpur, S. 2019 Global GRACE data assimilation for groundwater and drought monitoring: Advances and challenges. *Water Resources Research* **55**, 7564–7586.

Liang, X., Lettenmaier, D. P., Wood, E. F. & Burges, S. J. 1998 A simple hydrologically based model of land surface water and energy fluxes for general circulation models. *Journal of Geophysical Research: Atmospheres* **99**, 14415–14428.

Liu, B., Zou, X., Yi, S., Sneeuw, N., Cai, J. & Li, J. 2021 Identifying and separating climate- and human-driven water storage anomalies using GRACE satellite data. *Remote Sensing of Environment* **263**, 112559.

Long, D., Yang, Y., Wada, Y., Hong, Y., Liang, W. & Chen, Y. 2015 Deriving scaling factors using a global hydrological model to restore GRACE total water storage changes for China's Yangtze River Basin. *Remote Sensing of Environment* **168**, 177–193.

Luo, Z., Yao, C., Li, Q. & Huang, Z. 2016 Terrestrial water storage changes over the Pearl River Basin from GRACE and connections with Pacific climate variability. *Geodesy and Geodynamics* **7**, 171–179.

McCabe, G. J. & Wolock, D. 2013 Century-scale variability in global annual runoff examined using a water balance model. *International Journal of Climatology* **31**, 1739–1748. doi:10.1002/joc.2198.

Meng, F. C., Su, F. G., Li, Y. & Tong, K. 2019 Changes in terrestrial water storage during 2003–2014 and possible causes in Tibetan Plateau. *Journal of Geophysical Research: Atmospheres* **124**, 2909–2931.

Moghim, S. 2018 Impact of climate change on hydrometeorology in Iran. *Journal Global and Planetary Change* **170**, 93–105.

Ni, S., Chen, J., Jin, L., Chao, C. & Liang, Q. 2014 Terrestrial water storage changes in the Yangtze and Yellow River asins from grace time-variable gravity measurements. *Journal of Geodesy & Geodynamics* **34**, 49–54.

Nie, N., Zhang, W. C., Zhang, Z. J., Guo, H. D. & Ishwaran, N. 2016 Reconstructed terrestrial water storage change (ΔTWS) from 1948 to 2012 over the Amazon Basin with the latest GRACE and GLDAS products. *Water Resources Management* **30**, 279–294.

Ozdogan, M., Rodell, M., Beaudoing, H. K. & Toll, D. L. 2010 Simulating the effects of irrigation over the United States in a land surface model based on satellite-derived agricultural data. *Journal of Hydrometeorology* **11** (1), 171–184.

Pagliero, L., Bouraoui, F., Willems, P. & Diels, J. 2014 Large-scale hydrological simulations using the Soil and Water Assessment Tool, protocol development, and application in the Danube Basin. *Journal of Environmental Quality* 145–154. doi:10.2134/jeq2011.0359.

Pan, Y., Zhang, C., Gong, H. L., Yeh, P. J.-F., Shen, Y. J., Guo, Y., Huang, Z. Y. & Li, X. J. 2017 Detection of human-induced evapotranspiration using GRACE satellite observations in the Haihe River basin of China. *Geophysical Research Letters* **44**, 190–199.

Raghavendra, R. K. & Cholke, S. 2017 Assessment of watershed based water balance for irrigation scheduling through geospatial technique. *International Journal of Engineering Technology Science and Research (IJETSR)* **4** (8), 1128–1134.

Reager, J. T. & Famiglietti, J. S. 2009 Global terrestrial water storage capacity and flood potential using GRACE. *Geophysical Research Letters* **36**, L23402. doi:https://doi.org/10.1029/2009GL040826.

Reager, J. T., Thomas, B. F. & Famiglietti, J. S. 2014 River basin flood potential inferred using GRACE gravity observations at several months lead time. *Nature Geoscience* **7**, 588–592.

Reichle, R. H. & Koster, R. D. 2004 Bias reduction in short records of satellite soil moisture. *Geophysical Research Letters* **31** (19), L19501. https://doi.org/10.1029/2004GL020938.

Richey, A. S., Thomas, B. F., Lo, M.-H., Reager, J. T., Famiglietti, J. S., Voss, K., Swenson, S. & Rodell, M. 2015 Quantifying renewable groundwater stress with GRACE. *Water Resources Research* **51**, 5217–5238. doi: https://doi.org/10.1002/2015WR017349.

Rodell, M., Houser, P., Jambor, U., Gottschalck, J., Mitchell, K., Meng, C., Arsenault, K., Cosgrove, B., Radakovich, J., Bosilovich, M., Entin, J., Walker, J., Lohmann, D. & Toll, D. 2004 The global land data assimilation system. *Bulletin of the American Meteorological Society* **85** (3), 381–394.

Rodell, M., Chen, J., Kato, H., Famiglietti, J., Nigro, J. & Wilson, C. 2007 Estimating ground water storage changes in the Mississippi River basin (USA) using GRACE. *Hydrogeology Journal* **15**, 159–166.

Sathian, K. K. 2009 Application of GIS integrated SWAT model for basin level water balance. *Indian Journal of Soil Conservation* **37** (2), 100–105.

Scanlon, B. R., Zhang, Z., Save, H., Sun, A. Y., Müller Schmied, H., van Beek, L. P. H., Wiese, D. N., Wada, Y., Long, D., Reedy, R. C., Longuevergne, L., Döll, P. & Bierkens, M. F. P. 2018 Global models underestimate large decadal declining and rising water storage trends relative to GRACE satellite data. *Proceedings of the National Academy of Sciences U S A*. **115** (6), E1080–E1089. doi:10.1073/pnas.1704665115.

Seyoum, W. M. & Milewski, A. M. 2017 Improved methods for estimating local terrestrial water dynamics from grace in the northern high plains. *Adv. Water Resour. Res.* **110**, 279–290.

Seyoum, W. M., Kwon, D. & Milewski, A. M. 2019 Downscaling GRACE TWSA data into high-resolution groundwater level anomaly using machine learning-based models in a glacial aquifer system. *Remote Sensing* **11**, 824.

Singh, S. K., Saklani, B., Prakash, S., Chauhan, R. & Gupta, H. 2014 Geospatial approach for decentralized planning at Rajhana panchayat, Himachal Pradesh. *International Journal of Advancement in Remote Sensing, GIS and Geography* **2** (2), 27–43.

Singh, S. K., Mishra, S. K. & Kanga, S. 2017 Delineation of groundwater potential zone using geospatial techniques for Shimla city, Himachal Pradesh (India). *International Journal for Scientific Research and Development* **5** (4), 225–234.

Sun, Z., Long, D., Yang, W., Li, X. & Pan, Y. 2020 Reconstruction of GRACE data on changes in total water storage over the global land surface and 60 basins. *Water Resources Research* **56**, e2019WR026250.

Swenson, S. C. & Wahr, J. M. 2002 Methods for inferring regional surface-mass anomalies from Gravity Recovery and Climate Experiment (GRACE) measurements of time-variable gravity. *Journal of Geophysical Research: Solid Earth* **107**, 2193.

Swenson, S. & Wahr, J. 2006 Estimating large-scale precipitation minus evapotranspiration from GRACE satellite gravity measurements. *Journal of Hydrometeorology* **7**, 252–269.

Syed, T. H., Famiglietti, J. S., Rodell, M., Chen, J. L. & Wilson, C. R. 2008 Analysis of terrestrial water storage changes from GRACE and GLDAS. *Water Resources Research* **44**, W02433.

Tangdamrongsub, N., Hwang, C. & Kao, Y.-C. 2011 Water storage loss in central and south Asia from GRACE satellite gravity: Correlations with climate data. *Natural Hazards* **59**, 749–769.

Tao, S., Fang, J., Zhao, X., Zhao, S., Shen, H., Hu, H., Tang, Z., Wang, Z. & Guo, Q. 2015 Rapid loss of lakes on the Mongolian Plateau. *Proceedings of the National Academy of Sciences USA* **112**, 2281–2286.

Thomas, A. C., Reager, J. T., Famiglietti, J. S. & Rodell, M. 2014 A GRACE-based water storage deficit approach for hydrological drought characterization. *Geophysical Research Letters* **41**, 1537–1545.

Thompson, S. E., Harman, C. J., Troch, P. A., Brooks, P. D. & Sivapalan, M. 2011 Spatial scale dependence of ecohydrologically mediated water balance partitioning: A synthesis framework for catchment ecohydrology. *Journal of Water Resources Research* **47** (10), 143–158.

Tiri, A., Belkhiri, L., Asma, M. & Mouni, L. 2018 Suitability and assessment of surface water for irrigation purpose. We are IntechOpen, the world's leading publisher of Open Access books Built by scientists, for scientists. doi:10.5772/intechopen.86651.

Uniyal, B., Jha, M. K. & Verma, A. K. 2015 Assessing climate change impact on water balance components of a river basin using SWAT model. *Journal of Water Resources Management and Hydrology Process* **29** (13), 4767–4785.

Usmanov, S., Mitani, Y. & Kusuda, T. 2016 An integrated hydrological model for water balance estimation in the Chirchik River Basin, Northern Uzbekistan. *Journal of Computational Water, Energy, and Environmental Engineering* **5** (5), 87–97.

Vishwakarma, B. D., Horwath, M., Devaraju, B., Groh, A., Sneeuw, N. & Data-Driven, A. 2017 Approach for repairing the hydrological catchment signal damage due to filtering of GRACE products. *Water Resources Research* **53**, 9824–9844.

Wahr, J., Molenaar, M. & Bryan, F. 1998 Time variability of the earth's gravity field: Hydrological and oceanic effects and their possible detection using GRACE. *Journal of Geophysical Research: Solid Earth* **103**, 30205–30229.

Wang, K., Wang, P., Li, Z., Cribb, M. & Sparrow, M. 2007 A simple method to estimate actual evapotranspiration from a combination of net radiation, vegetation index, and temperature. *Journal of Geophysical Research Atmospheres* **112** (D15), D15107.

Wang, L. S., Chen, C., Ma, X., Fu, Z. Y., Zheng, Y. H. & Peng, Z. R. 2019 Evaluation of GRACE mascon solutions using in-situ geodetic data: The case of hydrologic-induced crust displacement in the Yangtze River Basin. *Science of the Total Environment* **707**, 135606.

Watkins, M. M., Wiese, D. N., Yuan, D. N., Boening, C. & Landerer, F. W. 2015 Improved methods for observing earth's time variable mass distribution with GRACE using spherical cap mascons. *Journal of Geophysical Research: Solid Earth* **120**, 2648–2671.

White, E. D., Easton, Z. M., Fuka, D. R., Collick, A. S., Adgo, E., McCartney, M., Awulachew, S. B., Selassie, Y. G. & Steenhuis, T. S. 2011 Development and application of a physically based landscape water balance in the SWAT model. *Journal of Hydrology Process* **25** (6), 915–925.

World Bank 2013 *Sub-Saharan Africa Annex: Sub-Saharan Africa Region Global Economic Prospects*. World Bank Group, Washington, D.C.

Xu, G., Liu, X., Zhang, Q. & Trouet, V. 2019 Century-scale temperature variability and onset of industrial-era warming in the Eastern Tibetan Plateau. *Climate Dynamics* **53**, 4569–4590.

Yang, T., Wang, C., Chen, Y., Chen, X. & Yu, Z. 2015 Climate change and water storage variability over an arid endorheic region. *Journal of Hydrology* **529**, 330–339.

Yang, P., Xia, J., Zhan, C., Qiao, Y. & Wang, Y. 2017 Monitoring the spatiotemporal changes of terrestrial water storage using GRACE data in the Tarim River basin between 2002 and 2015. *Science of the Total Environment* **595**, 218–228.

Yi, S., Sun, W., Chen, J. & Feng, W. 2016 *Anthropogenic and climate-driven water depletion in Asia*. Paper Presented AGU Fall Meeting 43, 9061–9069.

Yisehak, B., Shiferaw, H., Abrha, H., Gebremedhin, A., Hagos, H., Adhana, K. & Bezabh, T. 2021 Spatiotemporal characteristics of meteorological drought under changing climate in semi-arid region of northern Ethiopia. *Environmental Systems Research* **10**, 21. https://doi.org/10.1186/s40068-021-00226-4.

Yoshe, A. k. 2023 Estimation of change in terrestrial water storage for Abbay River Basin, Ethiopia. *Hydrology Research* **54** (11), 1451. doi:10.2166/nh.2023.119.

Zaitchik, B. F., Rodell, M. & Reichle, R. H. 2008 Assimilation of GRACE terrestrial water storage data into a land surface model: Results for the Mississippi River basin. *Journal of Hydrometeor* **9**, 535–548.

Zhao, K. & Li, X. 2017 Estimating terrestrial water storage changes in the Tarim River Basin using GRACE data. *Geophysical Journal International* **211**, 1449–1460.

Zhang, K., Kimball, J. S., Nemani, R. R., Running, S. W., Hong, Y., Gourley, J. J. & Yu, Z 2015 Vegetation greening and climate change promote multidecadal rises of global land evapotranspiration. *Scientific Reports* **5**, 1595.

Zhong, Y., Feng, W., Humphrey, V. & Zhong, M. 2019 Human-induced and climate-driven contributions to water storage variations in the Haihe River Basin, China. *Remote Sensing* **11**, 3050.

Zhou, X., Zhu, X., Dong, Z. & Guo, W. 2016 Estimation of biomass in wheat using random forest regression algorithm and remote sensing data. *The Crop Journal* **4**, 212–219.

First received 29 September 2023; accepted in revised form 8 February 2024. Available online 20 February 2024